



PEOPLE'S DEMOCRATIC REPUBLIC OF ALGERIA
Ministry of Higher Education and Scientific Research



University Amar Thelidji- Laghouat

Faculty of Technology

Department of Electronics

MASTER THESIS

Antar Nafissa Ilme

DOMAIN : Science & Technology

FIELD : Electronics

SPECIALTY : Instrumentation

Theme

***Design, Implementation and Control
of Flyback converter used for solar inverters***

Jury members:

| | | |
|-------------------------------|------------|----------------------|
| <i>Hadj Aissa Boubakeur</i> | <i>MCA</i> | President |
| <i>Oubbati Ibrahim Khalil</i> | <i>MCB</i> | Examiner |
| <i>ABOUCHABANA Nabil</i> | <i>MCB</i> | Supervisor |
| <i>AMEUR Khaled</i> | <i>MCB</i> | Co-supervisor |

2022/2023



PEOPLE'S DEMOCRATIC REPUBLIC OF ALGERIA
Ministry of Higher Education and Scientific Research



University Amar Thelidji- Laghouat

Faculty of Technology

Department of Electronics

MASTER THESIS

Aouissi Med Yacine

DOMAIN : Science & Technology

FIELD : Automation

SPECIALTY : Automation & Industrial Computing

Theme

***Design, Implementation and Control
of Flyback converter used for solar inverters***

Jury members

| | | |
|-------------------------------|------------|----------------------|
| <i>Hadj Aissa Boubakeur</i> | <i>MCA</i> | President |
| <i>Oubbati Ibrahim Khalil</i> | <i>MCB</i> | Examiner |
| <i>ABOUCBABANA Nabil</i> | <i>MCB</i> | Supervisor |
| <i>AMEUR Khaled</i> | <i>MCB</i> | Co-supervisor |

2022/2023

Acknowledgments

We are grateful to God for the health, willpower, courage, and determination that have been with us throughout the preparation and development of this project, allowing us to complete this humble endeavor.

We are deeply thankful to Ammar Telidji University, specifically the Faculty of Technologies and the Department of Electronics, for providing us the opportunity to successfully finish this project. Our heartfelt thanks go out to all our teachers and the individuals who tirelessly collaborated with us from the initial stages until the culmination of this research.

*We express our sincere appreciation to our supervisors, **Dr. Nabil Abouhabana** and **Dr. Ameer Khaled**, who have been extremely supportive throughout all stages of the research.*

We are sincerely grateful to the members of the jury for their valuable evaluation of our master thesis. Thank you for your time and expertise in assessing my work.

Lastly, we would like to express our heartfelt gratitude to our dear friends and family who have been incredibly supportive throughout the entire process of our work. We would also like to extend our thanks to all those who have contributed, near or far, to the successful completion of this graduation project. We are deeply grateful to Allah, the Magnificent and Ever Thankful, for His assistance and blessings. We firmly believe that without His blessings, this work would not have come to fruition.

Dedication

To my beloved and revered parents, no words can adequately convey the depth of my admiration, unwavering love, and profound gratitude for the immense sacrifices you have made to ensure my education and well-being. From the very beginning, you have showered me with unwavering support and boundless affection, guiding me on this journey of growth and knowledge. Your blessings have been my guiding light, and I am eternally grateful for your presence in my life.

Furthermore, I dedicate this humble achievement to my dear sister, brother, and all members of my cherished family. Your unwavering presence and unwavering support have been an unwavering source of strength throughout my endeavors. Your love, encouragement, and belief in me have fueled my determination to overcome challenges and reach new heights. With heartfelt appreciation, I thank you for always being by my side

Antar nafissa ilme

Dedication

I dedicate this master thesis to my parents, whose unwavering support and belief in my abilities have been the cornerstone of my academic journey. Your sacrifices and guidance have fueled my determination to succeed, this achievement is a testament to your love and unwavering belief in my potential.

I would also like to express my gratitude to my sisters, friends and loved ones who have stood by me throughout this journey. Your unwavering support, understanding, and encouragement have been invaluable. This thesis is dedicated to each of you, as your presence has been a source of inspiration and motivation.

AOUISSI mohammed yacine

Abstract :

Flyback converters are very popular in switch mode power supplies (SMPS) family, because of : its simplicity of design, its low cost, possibility to have a multiple isolated outputs, and its high efficiency. They are preferred especially for low power applications (< 150W). In this master's thesis we are presenting a comprehensive study on the design and control of a flyback converter. Our work begins with an in-depth exploration of the operating principles and components of the flyback. The design phase focuses on selecting suitable components and optimizing their parameters to achieve desired performance metrics, this addresses the implementation of the flyback converter, considering material selection and its control to ensure proper functionality and reliability.

Key word: SMPS, transformer, Flyback converter. magnetic core

Résumé :

Dans les alimentations à découpage (SMPS), les convertisseurs Flyback sont très populaires en raison de leur simplicité de conception, faible coût, possibilité d'avoir des sorties multiples et isolées et de leur rendement élevé. Ils sont privilégiés pour les faibles puissances (< 150 W). Dans cette thèse de master, nous nous présentons une étude approfondie sur la conception et la régulation d'un convertisseur Flyback. La thèse débute par une exploration approfondie sur les principes de fonctionnement et le choix des composants dans un convertisseur Flyback. La phase de conception se concentre sur la sélection de composants adaptés et l'optimisation de leurs paramètres afin d'atteindre des critères de performance souhaités. Elle aborde également la mise en œuvre du convertisseur Flyback, en tenant en compte la sélection des matériaux et de sa régulation afin d'assurer un fonctionnement adéquat.

Mots clés : Alimentation à découpage , transformateur, convertisseurs Flyback, noyau magnétique

ملخص:

في دوائر التغذية النبضية ، تُعتبر محولات الفلايباك (Flyback) شائعة جداً وهذا بسبب بساطة تصميمه، وتكلفته المنخفضة، مع إمكانية الحصول على عدة مخارج معزولة عن بعضها البعض، بالإضافة إلى مردوديته الطاقوية العالية. يُفضل استخدامها خصوصاً في التطبيقات ذات القدرة المنخفضة (150 واط). في أطروحة الماستر هذه، نقدم دراسة شاملة حول التصميم والتحكم في المحول Flyback. تبدأ الأطروحة باستكشاف مفصل لمبادئ التشغيل والمكونات الأساسية لمحول الفلايباك، بما في ذلك اختيار كل من : النواة المغناطيسية للمحول ومفتاح الطاقة، والصمام الثنائي. تركز مرحلة التصميم على اختيار العناصر المناسبة وتحسين معاييرها لتحقيق مقاييس الأداء المطلوب. تتناول أيضاً تطبيق الفلايباك مع مراعاة اختيار المواد المناسبة والتحكم اللازم لضمان الوظائف السليمة.

الكلمات المفتاحية: دوائر التغذية النبضية، المحول، محول فلاي باك.

Content

| | |
|--|-------------------|
| Content | <i>i</i> |
| List of figures | <i>iii</i> |
| List of tables | <i>v</i> |
| List of symbols | <i>vi</i> |
| List of abbreviation | <i>vii</i> |
| General introduction | <i>1</i> |
| CHAPTER I SWITCHING POWER SUPPLIES | <i>3</i> |
| I.1 INTRODUCTION | <i>4</i> |
| I.2 THE PRINCIPAL WORK OF SWITCHING POWER SUPPLIES | <i>4</i> |
| I.3 ADVANTAGES AND DISADVANTAGES OF SWITCHING POWER SUPPLIES..... | <i>5</i> |
| I.4 TYPES OF SWITCHING POWER | <i>5</i> |
| I.4.1 <i>Non isolated switching power supplies</i> | <i>5</i> |
| I.4.1.1 Step-up power supplies (boost chopper) | <i>5</i> |
| I.4.1.2 Step-down Power Supplies (buck chopper) | <i>5</i> |
| I.4.1.3 Buck-boost chopper | <i>6</i> |
| I.4.2 <i>Isolated switching power supplies</i> | <i>6</i> |
| I.4.2.1 Forward converter..... | <i>6</i> |
| I.4.2.2 Push pull converter | <i>7</i> |
| I.4.2.3 Full bridge converter | <i>8</i> |
| I.4.2.4 Half-bridge converter | <i>9</i> |
| I.4.2.5 Flyback converter | <i>9</i> |
| I.5 COMPARING ISOLATED AND NON-ISOLATED SWITCHING POWER SUPPLIES | <i>10</i> |
| I.6 CONCLUSION | <i>11</i> |
| CHAPTER II THEORETICAL STUDY OF FLYBACK CONVERTER | <i>12</i> |
| II.1 INTRODUCTION | <i>13</i> |
| II.2 FLYBACK CONVERTER CIRCUIT..... | <i>13</i> |
| II.2.1 <i>Description of components:</i> | <i>14</i> |
| II.3 THE PRINCIPLE OPERATION OF THE FLYBACK CONVERTER..... | <i>15</i> |
| II.4 EQUIVALENT CIRCUIT MODEL | <i>18</i> |
| II.5 TYPES OF CONDUCTION | <i>18</i> |
| II.5.1 <i>Continuous Conduction Mode (CCM)</i> | <i>18</i> |
| II.5.2 <i>Discontinuous Conduction Mode (DCM)</i> | <i>18</i> |
| II.6 ADVANTAGES AND DISADVANTAGES OF FLYBACK..... | <i>20</i> |

| | | |
|--|---|-----------|
| II.7 | APPLICATIONS OF FLYBACK CONVERTERS | 20 |
| II.8 | CONTROL AND PROTECTION MECHANISMS IN FLYBACK CONVERTERS | 21 |
| II.8.1 | <i>Snubber circuit</i> | 21 |
| II.8.2 | <i>The Feedback loop</i> | 22 |
| II.9 | CONCLUSION | 23 |
| CHAPTER III EXPERIMENTAL SETUP AND RESULTS..... | | 24 |
| III.1 | INTRODUCTION | 25 |
| III.2 | FLYBACK CONVERTER DESIGN AND COMPONENT SELECTION..... | 25 |
| III.2.1 | <i>Maximum primary inductance and turn ration calculation</i> | 26 |
| III.2.2 | <i>MOSFET selection</i> | 26 |
| III.2.3 | <i>Diode selection</i> | 27 |
| III.2.4 | <i>Snubber components selection</i> | 28 |
| III.2.5 | <i>Used components</i> | 28 |
| III.2.6 | <i>Core selection</i> | 30 |
| III.3 | SIMULATION..... | 32 |
| III.4 | EXPERIMENTAL SETUP | 38 |
| III.4.1 | <i>MOSFET driving circuit</i> | 38 |
| III.4.2 | <i>The results achieved through the realization</i> | 39 |
| III.4.2.1 | Open loop implementation | 40 |
| III.4.2.2 | Closed loop implementation | 42 |
| III.4.3 | <i>Test of control</i> | 54 |
| III.4.3.1 | Results of test 1 | 54 |
| III.4.3.2 | Results of test 2 | 56 |
| III.5 | CONCLUSION | 58 |

List of figures

| | |
|---|----|
| Figure I-1: Real photo of a switching power supplies | 4 |
| Figure I-2: Boost converter | 5 |
| Figure I-3: Buck converter | 6 |
| Figure I-4: Buck-Boost converter | 6 |
| Figure I-5: Forward converter circuit | 7 |
| Figure I-6: Push-pull converter | 8 |
| Figure I-7: Full-bridge circuit | 9 |
| Figure I-8: Half bridge converter circuit | 9 |
| Figure I-9: Flyback converter circuit | 10 |
| Figure II-1: Flyback converter multiple outputs | 13 |
| Figure II-2: Flyback converter with single out put | 14 |
| Figure II-3: Flyback converter during ON time | 15 |
| Figure II-4: Flyback converter during OFF time | 16 |
| Figure II-5: Flyback converter equivalent circuit model | 18 |
| Figure II-6: Chronogram of the continuous mode Flyback converter | 19 |
| Figure II-7: Chronogram of the discontinuous mode Flyback converter | 19 |
| Figure II-8 :Flyback converter with an input snubber circuit | 21 |
| Figure II-9: UC3843 | 22 |
| Figure II-10: Example for Flyback converter controlled with UC3844 | 23 |
| Figure III-1: STTH60L06W DIODE | 29 |
| Figure III-2: IRFP260M Transistor | 29 |
| Figure III-3: RHRG75120 Diode | 29 |
| Figure III-4: The specification input values | 30 |
| Figure III-5: The table of proposals cores 1 | 31 |
| Figure III-6: Ttable of proposals cores 2 | 31 |
| Figure III-7: ETD49 ferrite core | 32 |
| Figure III-8: choosing model window | 33 |
| Figure III-9: the PATH and the AREA parameters | 33 |
| Figure III-10: hysteresis curve table | 34 |
| Figure III-11: Magnetic curves of the ETD49 | 34 |
| Figure III-12: the hysteresis filled table | 35 |
| Figure III-13: The resultant Hysteresis curve | 35 |

| | |
|---|-----------|
| Figure III-14:Transformer selection..... | 36 |
| Figure III-15:properties of the transformer | 36 |
| Figure III-16:flyback converter circuit | 37 |
| Figure III-17:the simulation results..... | 37 |
| Figure III-18: real phto of realization..... | 38 |
| Figure III-19:Input voltage..... | 41 |
| Figure III-20:Output voltage | 41 |
| Figure III-21:Primary current | 42 |
| Figure III-22:Secondary current..... | 42 |
| Figure III-23:Dspace DS1103 | 52 |
| Figure III-24: Dspace Flyback converter diagram..... | 52 |
| Figure III-25:Functional diagram of HCPL 3120 | 39 |
| Figure III-26:HCPL 3120 | 39 |
| Figure III-27:Control of Flyback converter with simulink block | 54 |
| Figure III-28:Input voltage test 1..... | 55 |
| Figure III-29:Output voltage test 1 | 55 |
| Figure III-30:Duty cycle test 1..... | 56 |
| Figure III-31:Input voltage test 2..... | 57 |
| Figure III-32:Output voltage test 2..... | 57 |
| Figure III-33:Duty cycle test 2..... | 58 |

List of tables

| | |
|--|-----------|
| Table I-1 : Advantages and disadvantages of switching power supplies | 5 |
| Table I-2: comparative table between isolated switching power supplies and non-isolated switching power supplies..... | 10 |
| Tableau II-1: The difference between CCM and DCM | 20 |
| Tableau III-1: Design input summary | 25 |

List of symboles

A_L: Inductance factor

C_{sn}: snubber capacitor.

D:diode.

D_{max}: maximum duty cycle

F: Frequency.

I_c: capacitor current.

IC: isolated controller.

I_{PK}: maximum current the switch have to withstand.

I_{OUT} :the output current.

I_g:input current

K_{fr}: the ripple factor.

L_P :Primary Inductance.

N_s:secondary winding turns

N_p: primary winding turns

n:turn ratio.

η :efficiency.

Q1, Q2, Q3, Q4. : switchs.

R_c: resistance and capacitor.

R_{sn}: snubber resistance.

V_{D_{SMAX}}: maximum voltage the switch have to withstand.

V_{D_{1pk}} : maximum voltage the diode have to withstand.

V_g, V_{in}: input voltage.

V_L: voltage across the primary.

V_{out}, V: output voltage

V_{ref}: refence voltage.

V_{SN}: snubber voltage.

List of Abbreviation

DC : Direct Current

AC : Alternating Current

DC-DC: Direct Current to Direct Current.

SMPS: Switching Mode Power Supplies

DCM: Discontinuous Conduction Mode

CCM: Continuous Conduction Mode

PWM: Pulse Width Modulation

RCP: rapid control prototyping

*General
introduction*

Switched mode power supplies (SMPS) have gained popularity over the years due to their numerous advantages. These include their compact size, lightweight design, high efficiency, and consequently low heat dissipation. These qualities make them highly sought after in various industries and applications. The use of switched mode power supplies continues to grow as they provide an optimal balance between performance and energy conservation. [1]

SMPS find numerous applications in many fields such as electronics, telecommunications and medical devices and commercial solar inverters. the SMPS classification is based on the relationship between the input voltage and the output voltage and there design if it's with transformer or without it such as step-down (buck), step-up (boost), and buck-boost , All other configurations like the Flyback (magnetic energy storage), forward (direct conduction), push-pull and full-bridge are derived from these basic configurations.

Flyback converters are one of the most commonly used switching power supplies in low power applications where the output voltage needs to be isolated from the main input power supply [2].

In Flyback converter design, the transformer is crucial for determining performance, including efficiency and output regulation. The transformer's characteristics directly impact these aspects, making proper selection and design paramount. Efficient power conversion and reliable operation rely on the transformer's efficiency and ability to regulate the output voltage. Careful consideration and design of the transformer are vital for achieving desired performance in Flyback converters.

The type of the core of the transformer should be well chosen regarding to system requirements including number of outputs, physical height, cost and so on , Ferrite is the most widely used core material for commercial SMPS application [3].

The control of a Flyback converter involves regulating the output voltage by manipulating the switching action of the power semiconductor device. This is typically achieved through pulse width modulation (PWM) techniques, where the duty cycle of the switch is adjusted to control the energy transfer to the output.

Due to its non-linear characteristics, similar to other switching converters, the Flyback converter poses challenges in controller design, necessitating the use of a non-linear controller to achieve satisfactory dynamic and steady-state performance. Additionally, robust behavior is crucial for these circuits, ensuring minimal sensitivity to variations in input voltage, parameters,

or load conditions. Furthermore, the presence of steady-state faults presents an additional concern for control circuits [4].

The purpose of this study is to present a comprehensive study on the design and control of Flyback converters and to optimize the Flyback converter in the terms of efficiency, reliability and power conversion for solar energy applications

The written thesis pertaining to this work is organized into three chapters:

The first chapter of this thesis provides an overview of switching mode power supplies, focusing on their principles and various types, including the Flyback configuration. In this section, general information are presented to familiarize readers with the fundamental concepts and characteristics of switching mode power supplies.

In the second chapter, we extensively explore the modeling of Flyback converters, encompassing various aspects such as conduction modes, constituent components, and a comprehensive analysis of their advantages and disadvantages. This chapter delves deeper into the intricacies of Flyback converter operation

The third chapter delves into the practical aspects of the design process, where careful consideration is given to selecting the appropriate components and implementing a control scheme that ensures the desired output voltage stability at the specified value of 12V.

Chapter I

Switching power supplies

I.1 Introduction

Switching power supplies are direct current direct current (DC-DC) converters which make it possible to supply a variable direct voltage, from a constant DC voltage source obtained in almost cases from a rectified and filtered alternating source. Switching power supplies include a transformer providing galvanic isolation between the output and the input voltage. This transformer allows lowering or raising the output voltage according to the transformation ratio.

Switching power supply technology is based on voltage-control using power electronics components such as IGBT or MOSFET transistors operating in switching mode. [5]

Switching power supplies are widely used in electronic devices PC, TV, measuring devices and in telecommunication centers. In last years they are also used in commercial solar inverters.



Figure I-1: Real photo of a switching power supplies

I.2 The principal work of switching power supplies

The principles of switching power supplies revolve around the efficient conversion of electrical power.

- The input AC voltage is rectified and filtered to obtain a pulsating DC voltage.
- The pulsating DC voltage is rapidly switched on and off at a high frequency using a power semiconductor device.
- The high-frequency voltage pulses are applied to a transformer for efficient energy transfer.
- The transformer output is rectified and filtered to obtain a smooth DC voltage.
- The output voltage is measured, compared to a reference voltage, and used to adjust the switching to regulate the output voltage [6].

I.3 Advantages and disadvantages of switching power supplies

This table represent the advantages And the disadvantages of the switching power supplies:

Table I-1 : Advantages and disadvantages of switching power supplies

| <i>Advantages</i> | <i>Disadvantages</i> |
|------------------------------------|------------------------------|
| Low losses | Noise and ripple |
| Excellent yield ($\eta > 80 \%$) | Complex design |
| Compact Size and Light Weight | Electromagnetic interference |

I.4 Types of switching power

In literature there are many structure of a DC-DC converters (SMPS) which we can divided them to two big categories :

I.4.1 Non isolated switching power supplies

The input source and the output load share a common current path during operation and energy is transferred through energy storage elements (Inductors & Capacitors) [7].

In this category we find :

I.4.1.1 Step-up power supplies (boost chopper)

Boost converter is a fundamental dc–dc voltage step-up circuit with several features that make it suitable for various applications in products ranging from low-power portable devices to high-power stationary applications [8]. its circuit is shown in the figure below:

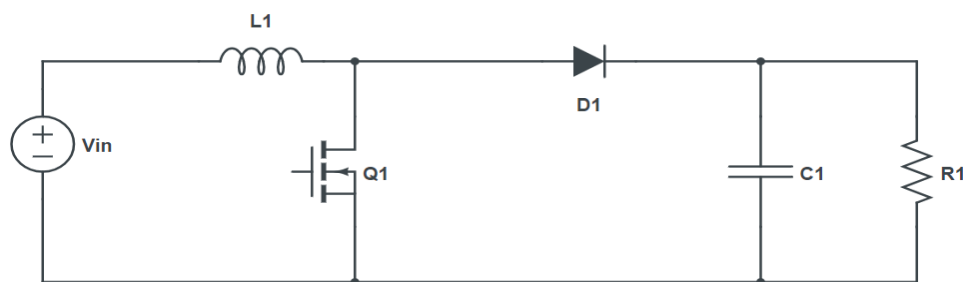


Figure I-2: Boost converter

I.4.1.2 Step-down Power Supplies (buck chopper)

The step-down converter is often referred to in the literature as a buck converter which is a switch, can only connect two sources of different current/voltage types or vice versa. Its typical application is to convert its input voltage to a lower output voltage [9]. its circuit is shown in the figure below:

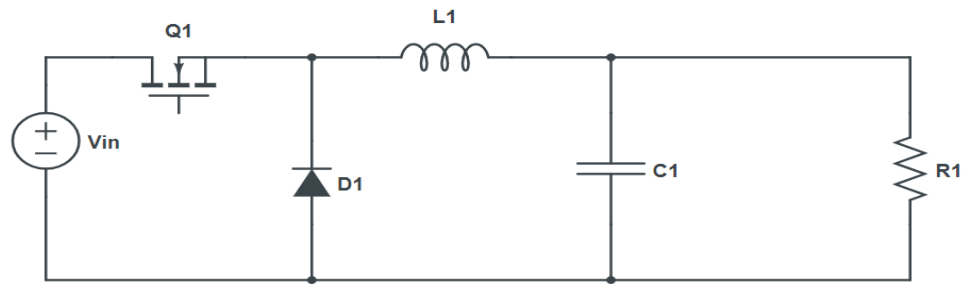


Figure I-3: Buck converter

I.4.1.3 Buck-boost chopper

The main application of a step-down step-up or buck-boost converter is in regulated dc power supplies, where a negative-polarity output may be desired with respect to the common terminal of the input voltage, and the output voltage can be either higher or lower than the input voltage. A buck - boost converter can be obtained by the cascade connection of the two basic converters: the step-down converter and the step-up converter [10]. its circuit is shown in the figure below:

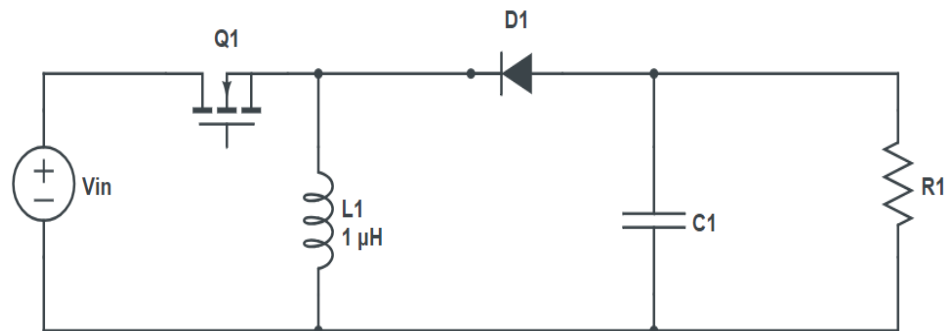


Figure I-4: Buck-Boost converter

I.4.2 Isolated switching power supplies

This types of switching power supplies transfer the energy by coupled magnetic components usually a transformer while providing isolation between the input and the output voltage, in this type there are many of switching power supplies :

I.4.2.1 Forward converter

A forward converter is a type of power electronics converter used in a variety of applications, especially power supply designs. This is a transformer-isolated converter that performs step-down voltage conversion.

The basic topology of a forward converter includes a transformer, two switches (usually power transistors or MOSFETs), a diode, an output inductor, and a capacitor. Transformers play an important role in converter operation.

During operation, one of the switches, called the primary switch, is turned on, allowing current to flow through the primary winding of the transformer. This current causes energy to be stored in the core of the transformer. When the primary switch is turned off, the energy stored in the transformer is transferred to the secondary winding. The secondary side consists of the output diode, inductor and capacitor. Energy is transferred by magnetizing currents in transformers. The diode allows current to flow from the secondary winding of the transformer to the output inductor and capacitor, producing a step-down voltage at the output. Inductors and capacitors help filter and regulate the output voltage.

A forward converter operates in continuous or discontinuous mode depending on the load conditions. In continuous operation, the current in the primary winding of the transformer never reaches zero during a complete switching cycle. In discontinuous mode, the primary current drops to zero before the next switching cycle begins.

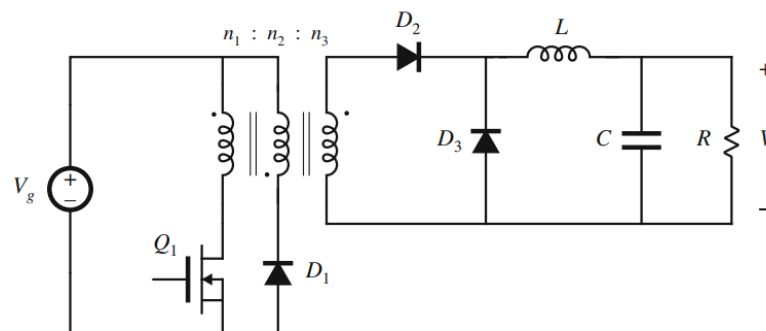


Figure I-5: Forward converter circuit

1.4.2.2 Push pull converter

A push-pull converter is a type of power electronics converter that allows voltage step-up or step-down conversion. Commonly used in power supply applications to efficiently convert DC voltages.

The basic topology of a push-pull converter consists of a center-tapped transformer, two switches (usually power transistors or MOSFETs), and two diodes. Transformers are important components that enable energy transfer and voltage conversion.

During operation, the two switches alternate on and off in a complementary manner. When the switch is turned on, current flows through the primary winding of the transformer. This current causes energy to be stored in the core of the transformer. When this switch is off,

the energy stored in the transformer is transferred to the secondary winding through a diode connected to one end of the secondary winding. At the same time, the other switch turns on, allowing current to flow in the opposite direction through the primary winding. This process is called a converter because it is repeated in a push-pull process. A diode connected to the other end of the secondary winding conducts during the on-time of the other switch, completing the energy transfer. The output voltage of a push-pull converter is determined by the turns ratio of the transformer. If there are many turns on the secondary side of the transformer, the output voltage will be higher than the input voltage, resulting in a step-up.

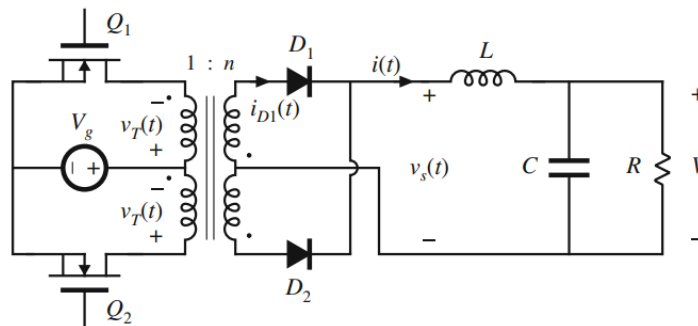


Figure I-6: Push-pull converter

1.4.2.3 Full bridge converter

A full-bridge converter is a type of power electronics converter used in a variety of applications such as power supplies, motor drives, and renewable energy systems. This is a four-switch converter that uses four power electronic switches arranged in a bridge configuration.

The basic topology of a full-bridge converter consists of four switches, usually composed of power transistors or insulated gate bipolar transistors (IGBTs), connected in a bridge configuration. The switches are usually called Q1, Q2, Q3, Q4. The load is connected between his two nodes of the bridge. During operation, the switch is controlled to allow current flow in either direction through the load. By controlling the switching of each switch, the output voltage and output current can be adjusted and controlled.

When operating a full-bridge converter, the diagonal switches of the bridge are switched on and off complementarily. For example, if switches Q1 and Q4 are on and switches Q2 and Q3 are off, current will flow from the input to the output through the load. Changing the state of the switch changes the direction and magnitude of the current.

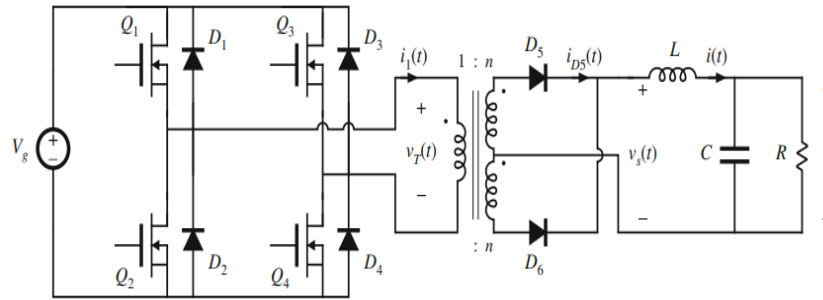


Figure I-7: Full-bridge circuit

1.4.2.4 Half-bridge converter

Half-bridge converters are another type of power electronics converter commonly used in various applications such as motor drives, power supplies, and inverters. This is a two-switch converter consisting of two power electronic switches connected in a half-bridge configuration.

The basic topology of a half-bridge converter consists of two switches usually power transistors or IGBTs connected in series with a load. The midpoint between the switches is usually connected to the DC power supply.

During operation, the switches are controlled complementary. When one switch is on, the other switch is off. By changing the state of the switch, you can control the direction and magnitude of the current through the load.

For example, if the top switch is on and the bottom switch is off, current will flow from the DC source through the top switch, the load, and back to the DC source. Reversing the state of the switch reverses the direction of current flow.

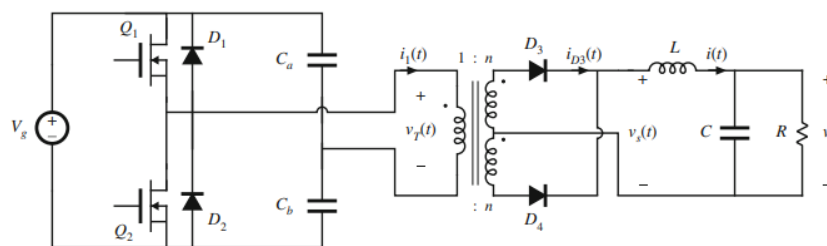


Figure I-8: Half bridge converter circuit

1.4.2.5 Flyback converter

Flyback converter is a very practical isolated version of the buck–boost converter. The inductor of the buck–boost converter has been replaced by a Flyback transformer. The dc input source V_g and the switch Q_1 are connected in series with the primary transformer. The diode D_1

and the RC output circuit are connected in series with the secondary of the Flyback transformer [11].

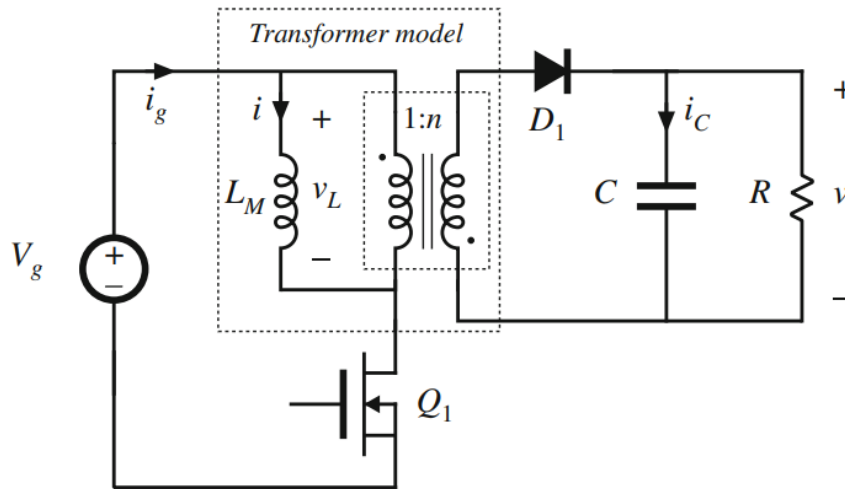


Figure I-9:Flyback converter circuit

I.5 Comparing Isolated and Non-Isolated Switching Power Supplies

the performance and characteristics of switching power supplies can vary depending on specific designs, implementations, and manufacturers. The following table is intended to provide a broad comparison between isolated and non-isolated switching power supplies, but it may not capture all the nuances of individual products:

Table I-2: comparative table between isolated switching power supplies and non-isolated switching power supplies

| | Isolated switching power supplies | Non-isolated switching power supplies |
|---------------------------|---|---|
| Voltage conversion | Capable of converting voltage up or down | Primarily converts voltage down to a lower level |
| Application | Suitable for sensitive or high-voltage applications | Typically used in low-voltage applications |
| Safety | Offers protection against electric shocks | Lower safety level due to lack of isolation |
| Efficiency | Higher efficiency if its well controlled | Higher efficiency due to the absence of isolation |
| Size and cost | Generally larger in size and more expensive | Generally smaller in size and less expensive |

I.6 Conclusion

This chapter provides an overview of switching power supplies, including a concise description of their types and associated circuits. It also discusses the advantages and limitations of switching power supplies, highlighting their key principles. Furthermore, it presents a comparative study between isolated switching power supplies and non-isolated switching power supplies, allowing for a comprehensive understanding of the various design approaches and methodologies employed in studying the operation of these converter types.

In the upcoming chapter of our thesis, we will focus on the Flyback converter, offering a comprehensive exploration of its theoretical study, design considerations, and mathematic modeling .

Chapter II

Theoretical study of flyback converter

II.1 Introduction

DC-DC converters play a crucial role in power electronics, prompting researchers to focus on enhancing converter efficiency [12]. Among various topologies utilized in low-power applications, the Flyback converter stands out due to its relative simplicity. Due to their affordability, simple design, and efficient performance, Flyback converters are widely utilized in Switching Mode Power Supply (SMPS) systems. These converters are favored for their ability to provide multiple isolated outputs and achieve high output voltages. Additionally, they are renowned for their excellent efficiency, making them a popular choice in various applications that require reliable power supply.

In Flyback converters, a transformer is used for energy storage, input-output isolation, and output power transformation.

Flyback transformers are meticulously designed with specific polarities in their windings to ensure precise control of current flow. This polarity arrangement guarantees that when current is directed through one winding, the other winding remains isolated and unaffected. By carefully managing the polarity of the windings, the Flyback converter can efficiently transfer energy between the primary and secondary sides without undesired current interactions. This crucial design aspect enables the Flyback transformer to function effectively in its intended application, providing reliable power conversion and isolation [13].

II.2 Flyback converter circuit

One of the advantages of the Flyback converter is that it can have one or several outputs as shown in the figure II-1.

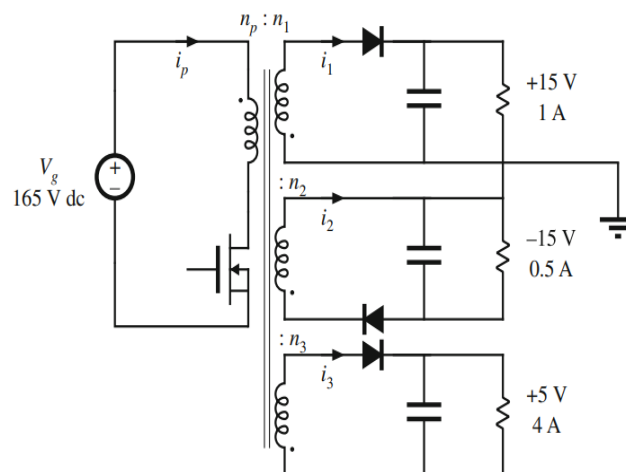


Figure II-1: Flyback converter multiple outputs

The multiple-outputs switching converter is generally used in low power applications for electronic equipment that need different levels of output voltages such as computers [14].

These outputs can be either positive or negative, and this helps a lot in electronic applications, such as feeding several circuits at one time that why it is the most used.

In our work , we will discuss a Flyback with one output voltage.

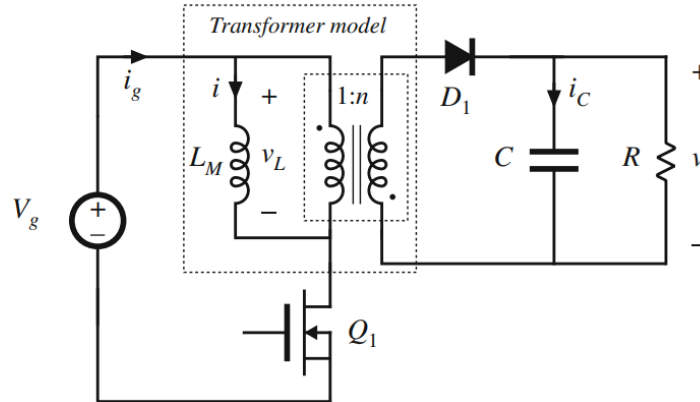


Figure II-2: Flyback converter with single out put

II.2.1 Description of components:

Switch(Q_1): A switch is used to control the current through the primary winding of a transformer. It is usually a MOSFET whose duty cycle is controlled to regulate the output voltage.

Diode(D_1): The diode is used to provide a path for the current flow during the OFF state of the switch. It is typically a fast-recovery or ultrafast diode, and its reverse-recovery characteristics are important to minimize losses.

Transformer: The transformer is the key component of the Flyback Converter. It is used to store energy in its magnetic field when the switch is ON, and release it when the switch is OFF, resulting in a stepped-down voltage at the output. The transformer also provides galvanic isolation between the input and output, which can be important in some applications.

Output Filter(C): The output filter consists of a capacitor, which is used to smooth out the output voltage and filter out any remaining switching noise. The value of the capacitor must be carefully selected to provide the desired filtering characteristics.

Control Circuitry: The Flyback Converter requires control circuitry to regulate the output voltage and control the duty cycle of the switch. This circuitry typically consists of a controller

IC or a microcontroller, which uses feedback from the output to adjust the duty cycle of the switch.

Together, these components provide a simple, efficient, and cost-effective method of DC-DC conversion.

II.3 The Principle operation of the Flyback converter

The operating principle of the Flyback Converter is based on the transfer of energy between the primary and secondary windings of the transformer.

When the switch is ON, current flows through the primary winding of the transformer, storing energy in the core's magnetic field. At the same time, the diode is reverse biased which prevents current from passing through the secondary winding [15].

The equivalent circuit of this period is presented in figure II-3

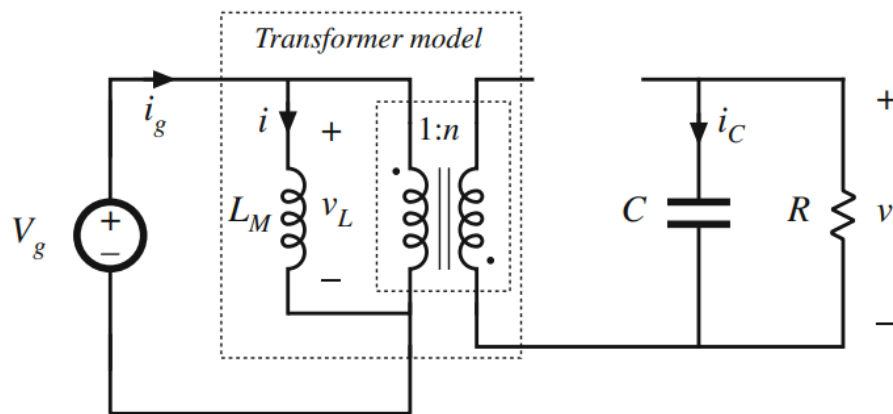


Figure II-3: Flyback converter during ON time

Switch ON : $0 < t < DT$

V_L the primary winding voltage during the ON time :

$$V_L = V_g \quad \text{Equation II-1}$$

I_C the flowing current in the output capacitor during the ON time:

$$i_c = -\frac{V}{R} \quad \text{Equation II-2}$$

I_g the input current during the ON time :

$$i_g = i$$

Equation II-3

When the switch is turned OFF, the magnetic field collapses, energizing the secondary winding. The diode becomes forward biased, allowing current to pass through the secondary winding to the output filter. As a result of this current discharge, the voltage at the output decreases.

The equivalent circuit of this period is presented in figure II-4

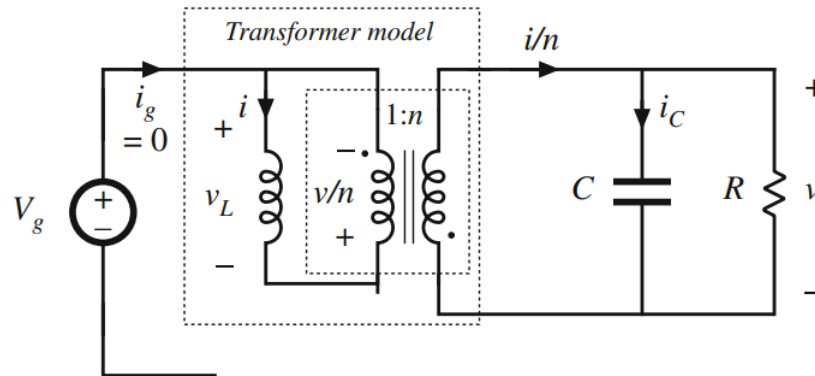


Figure II-4: Flyback converter during OFF time

Switch OFF: $DT < t < T$

V_L the primary winding voltage during the OFF time

$$V_L = -\frac{V}{n} \quad \text{Equation II-4}$$

I_C the flowing current in the output capacitor during the OFF time:

$$i_c = \frac{i}{n} - \frac{V}{R} \quad \text{Equation II-5}$$

I_g the input current during the OFF time :

$$i_g = 0 \quad \text{Equation II-6}$$

The voltage conversion ratio is determined by the turns ratio of the transformer, which can be designed to produce the desired output voltage. The duty cycle of the switch is controlled to regulate the output voltage with a higher duty cycle resulting in a higher output voltage [15].

In the steady state we combine the equations obtained during the two periods ON and OFF:

For V_L we have the following equation:

$$\langle VL \rangle \geq 0 \Leftrightarrow Vg * D - \frac{V}{n} * (1 - D) = 0 \quad \text{Equation II-7}$$

Solution for the conversion ratio then leads to:

$$Vg * D = \frac{V}{n} * (1 - D) \quad \text{Equation II-8}$$

$$\frac{V}{Vg} = \frac{D * n}{1 - D} \quad \text{Equation II-9}$$

We remark that the conversion ratio of the Flyback converter is similar to that of the buck–boost converter, but contains an added factor of n.

For i_c we have :

$$\langle i_c \rangle = 0 \Leftrightarrow -\frac{V}{R} * D + \left(\frac{i}{n} - \frac{V}{R}\right) * (1 - D) = 0 \quad \text{Equation II-10}$$

$$-\frac{V}{R} * D + \frac{i}{n} * (1 - D) - \frac{V}{R} + \frac{V}{R} * D = 0 \quad \text{Equation II-11}$$

After simplifying the equation:

$$\frac{i}{n} * (1 - D) - \frac{V}{R} = 0 \quad \text{Equation II-12}$$

$$\frac{i}{n} * (1 - D) = \frac{V}{R} \quad \text{Equation II-13}$$

Solution of i yields :

$$i = \frac{V * n}{R * (1 - D)} \quad \text{Equation II-14}$$

for i_g yields :

$$i_g = \langle i_g \rangle = 0 \Leftrightarrow i * D + 0 * (1 - D) = D * i \quad \text{Equation II-15}$$

II.4 Equivalent circuit model

An equivalent circuit that models the dc components of the Flyback converter waveforms can now be constructed. Circuits corresponding to the inductor loop equation (II.7) and to node equations (II.10) and (II.15) are illustrated in figure II-5 .

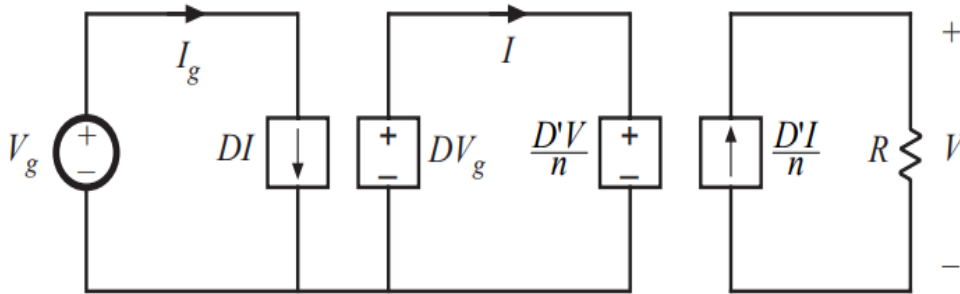


Figure II-5: Flyback converter equivalent circuit model

II.5 Types of conduction

Several factors, including power level, load conditions, and desired efficiency, influence the selection of the conduction mode. The choice of conduction mode depends on these variables and determines the most optimal mode of operation for achieving the desired performance.

II.5.1 Continuous Conduction Mode (CCM)

If the current is greater than zero when the Toff time is complete, this operation is defined as continuous conduction mode (CCM) [16].

This mode often the preferred choice for higher power levels due to its ability to minimize switching losses. In CCM, the current flows continuously through the inductor, resulting in lower power dissipation during switching transitions. As a result, CCM exhibits higher efficiency and is well-suited for high-power applications

II.5.2 Discontinuous Conduction Mode (DCM)

The Flyback converter has the capability to operate in two distinct modes depending on certain conditions. One of these modes is known as the discontinuous conduction mode (DCM). In this mode, if the secondary current drops to zero before the completion of the Toff time, the converter operates in a discontinuous manner. This discontinuous conduction mode occurs as a result of specific operating conditions within the Flyback converter [16].

This mode often preferred for lower power applications. In DCM, the inductor current drops to zero during a portion of each switching cycle, resulting in reduced switching stress. This

mode allows for improved efficiency at lighter loads since there is less energy wasted during switching transitions. DCM is suitable when the power level is lower and achieving higher efficiency during lighter load conditions is desirable.

The following figures represents the two types of conduction the DCM and CCM :

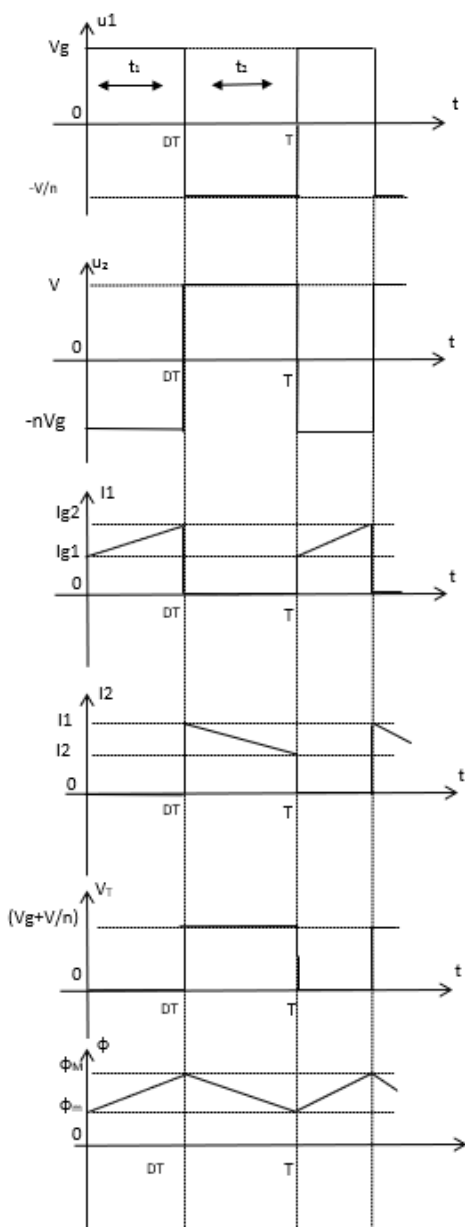


Figure II-6: Chronogram of the continuous mode Flyback converter

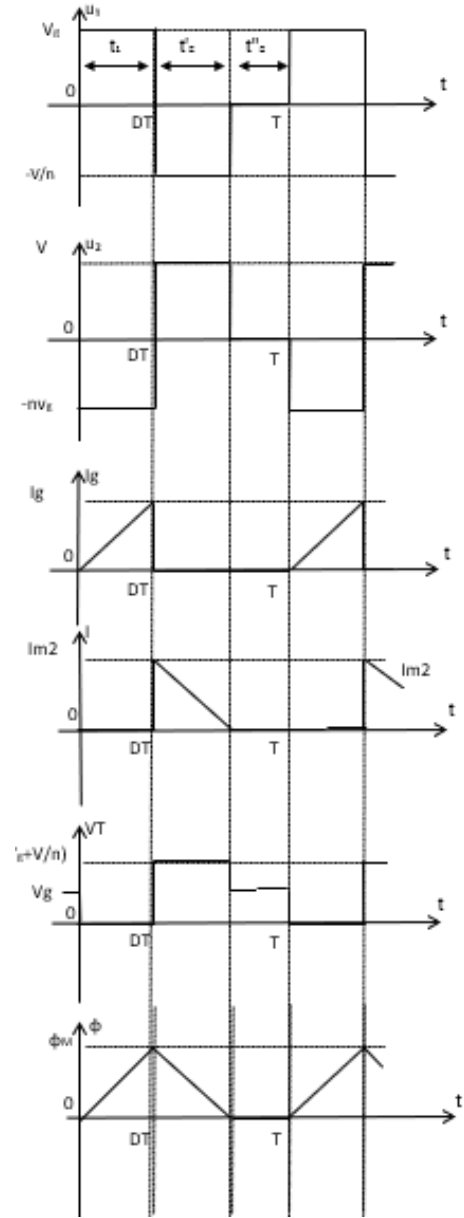


Figure II-7: Chronogram of the discontinuous mode Flyback converter

Understanding the differences between CCM and DCM is crucial for designing and optimizing the performance of Flyback converters in various applications.

The following table summarize the key differences between Continuous Conduction Mode (CCM) and Discontinuous Conduction Mode (DCM) in Flyback converters:

Table II-1: The difference between CCM and DCM

| | CCM | DCM |
|------------------|---|---|
| Current waveform | Current never reaches zero during switching cycle | Current drops to zero before the end of the cycle |
| Switching losses | Lower switching losses | Reduced switching stress |
| Efficiency | Efficient at higher loads | Improved efficiency at lighter loads |
| Application | Suitable for high-power applications | Improved efficiency at lighter loads |
| Size | Large core of transformer | Small core of transformer |

II.6 Advantages and disadvantages of flyback

The Flyback Converter has several advantages:

- Regulation of the multiple output voltages with a single control.
- The primary is isolated from the output.
- Capable to supply multiple output voltages all isolated from the primary.
- A use of very few components compared to the other types of SMPSs [17].

The disadvantages of application of Flyback converter:

- Flyback converter require additional snubber circuit to overcome leakage current of inductor [18].
- More output and input capacitance [19].
- Higher losses.
- has poor efficiency and is a pulsating source current.

II.7 Applications of Flyback converters

The Flyback Converter can be used in a wide range of applications [17]:

- LED lighting.

- battery chargers.
- High-voltage supplies in TV and Monitor CRTs.
- Lasers, Xenon ,flashlights.
- data center power supplies.
- Solar inverters.

II.8 Control and Protection Mechanisms in Flyback Converters

Both the snubber circuit and the feedback loop contribute to the proper functioning and performance of Flyback converters by addressing voltage spikes and providing control mechanisms for stable and regulated output operation.

II.8.1 Snubber circuit

Power semiconductors are the heart of power electronics equipment. Snubbers are circuits which are placed across semiconductor devices for protection and to improve performance. Snubbers can do many things : Reduce or eliminate voltage or current spikes, Reduce total losses due to switching, Transfer power dissipation from the switch to a resistor or a useful load [20].

There are many different kinds of snubbers but the two most common ones are the resistor-capacitor (RC) damping network and the resistor-capacitor-diode (RCD) turn-off snubber .usually flyback converters uses RCD circuit .

When the MOSFET turns off, a high-voltage spike occurs on the drain pin because of a resonance between the leakage inductor of the main transformer and the output capacitor of the MOSFET. The excessive voltage on the drain pin may lead to an avalanche breakdown and eventually damage the MOSFET. Therefore, it is necessary to add an additional circuit to clamp the voltage [21].

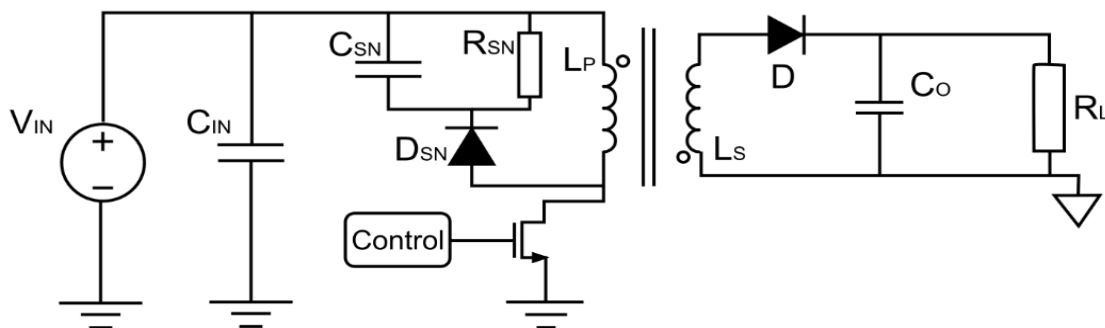


Figure II-8 :Flyback converter with an input snubber circuit

II.8.2 The Feedback loop

The feedback loop is a critical component of Flyback converters, responsible for regulating the output voltage and ensuring stable operation. It monitors the output voltage, compares it to a reference value, and adjusts the duty cycle of the switching transistor accordingly. This adjustment controls the energy transfer from input to output, maintaining the desired output voltage.

In a typical Flyback converter feedback loop, the output voltage is sensed using a voltage sensor. A feedback error amplifier compares the sensed voltage to a reference voltage, generating an error signal representing the voltage difference. The controller processes this signal and modulates the duty cycle of the switching transistor. By providing stability and accuracy, the feedback loop allows the Flyback converter to handle load variations, input voltage fluctuations, and other operating conditions. It compensates for disturbances, ensuring proper voltage regulation. The feedback loop plays a crucial role in achieving reliable operation and efficient power delivery. Overall, the feedback loop is essential for maintaining the desired output voltage, adapting to system changes, and ensuring efficient operation in Flyback converters.

The UC3842/UC3843/UC3844/UC3845 are fixed frequency current-mode PWM controller, its specially designed for Off-Line and DC to DC converter applications with minimum external components. This integrated circuit feature a trimmed oscillator for precise duty cycle control, a temperature compensated reference, high gain error amplifier, current sensing comparator and a high current totem pole output for driving a Power MOSFET [22].

The Flyback converter is generally commanded with UC3843.

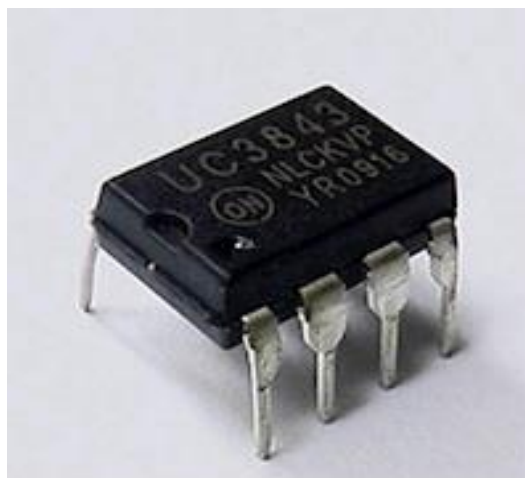


Figure II-9: UC3843

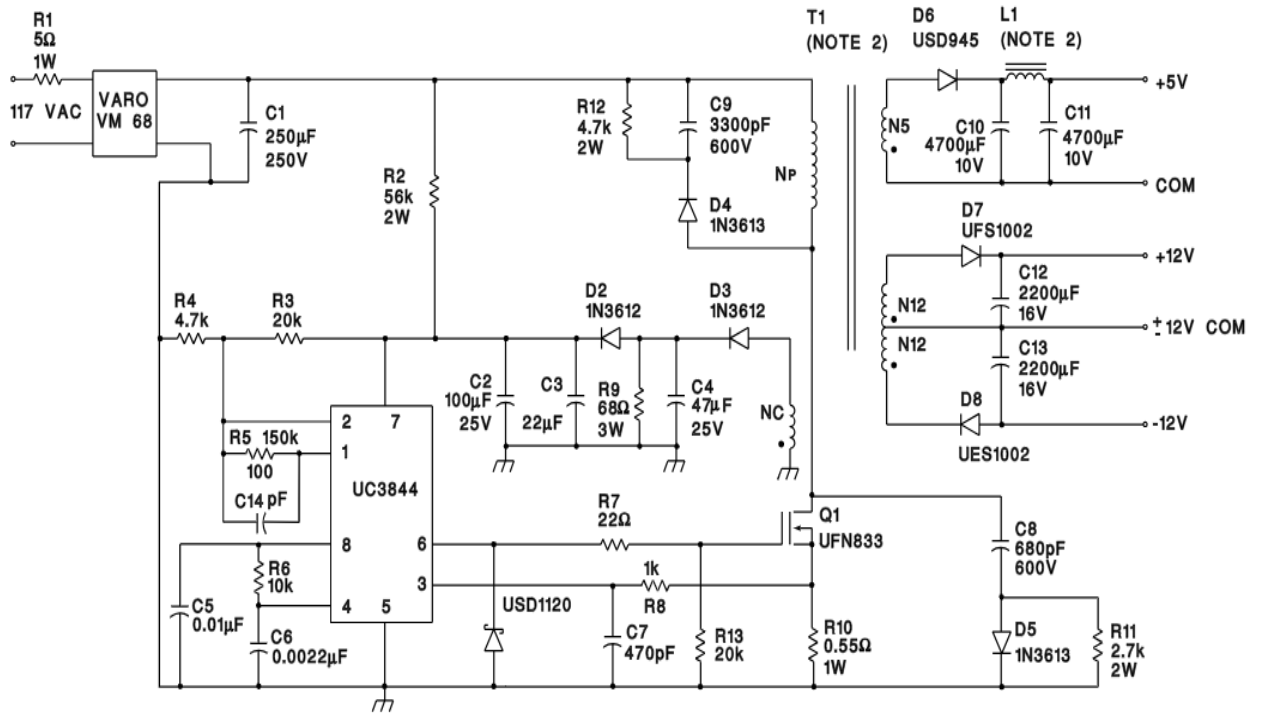


Figure II-10: Example for Flyback converter controlled with UC3844

II.9 Conclusion

The primary aim of the second chapter was to introduce the Flyback converter, a promising solution with great potential to fulfill our needs, particularly in electronics. This chapter delves into the operational principles, component description, and primary conduction modes (CCM and DCM) of the Flyback converter.

Moreover, it explores the behavior of the converter, shedding light on the transfer of voltage from the primary winding to the secondary winding, as well as the development of the magnetic field when current starts to flow.

Following the introduction to the fundamental concepts of Flyback converters, the subsequent chapter focuses on delving deeper into transformer designs. With an aim to provide a comprehensive understanding of the topic, next chapter explores various aspects related to the design of converter specifically Flyback converters by delving into the intricacies of converter design.

Chapter III

Experimental setup and results

III.1 Introduction

The aims of this chapter are: design, realization and practical implementation of the Flyback converter, including component selection, assembly, testing, and performance evaluation. It ensures that the theoretical design is translated into a functional and reliable power electronic system.

The Flyback topology is one of the most SMPS frequently used. Although simple, this converter design offers great advantages for certain applications. New, more complex topologies have surfaced in recent years, but Flyback converters remain a popular design choice.

The section of the transformer study is an important part that determines the efficiency performance, output voltage regulation and electromagnetic interference for Flyback converters. The transformer of the Flyback converter is inherently an inductor that is used for energy storage and isolation contrary to the classical power transformer. In the general transformer, the current flows in both the primary and secondary winding at the same time. However, in the Flyback transformer, the current flows only in the primary winding while the energy in the core is charged and in the secondary winding while the energy in the core is discharged. Usually, gap is introduced between the core to increase the energy storage capacity [23].

III.2 Flyback Converter Design and Component Selection

To design the Flyback converter, several specification are taken in consideration. In this contest we mention, required input voltage, output voltage, power levels and the conduction mode. This information will help us in the selection of components and design process.

The following table presents the specifications of our converter:

Table III-1: Design input summary

| Design parameters | value |
|----------------------------------|--------|
| Input voltage (V_{IN}) | 20-30v |
| Output voltage (V_{OUT}) | 12v |
| Output current (I_{OUT}) | 2A |
| Switching frequency (F) | 30Khz |
| Estimated efficiency (η) | 100% |
| Maximum duty cycle (D_{MAX}) | 0.5 |
| Operation mode | DCM |

In order to ensure the performance and safety of the circuit, it is essential to undertake thorough calculations and component selection. To determine and select the perfect components in order to carry out our Flyback converter, we will delve into each step to design the Flyback converter. This components are: MOSFET ,Diode , the Maximum Primary Inductance, the turn ratio and the snubber circuit.

III.2.1 Maximum primary inductance and turn ration calculation

There are many ways to Select the Maximum Primary Inductance L_p . In our case, the converter is operating in DCM conduction mode.

Discontinuous conduction mode (DCM) was selected for this application due to its increased stability and higher efficiency. This means that the solution ripple factor (K_{rf}) equal to 1.

Calculation of the L_p is obtained by equation II.1 [24]

$$L_p = \frac{\eta \times D_{max}^2 \times V_{in}^2}{2 \times F \times K_{rf} \times P_o} \quad \text{Equation III-1}$$

Numerical application:

$$L_p = 100\mu\text{h}$$

With: D_{MAX} is the maximum duty cycle, V_{in} is the input voltage, P_o is the output power, F is the switching frequency, K_{rf} is the ripple factor.

Next, the required turn ratio (n) is calculated by applying V_{in} and maximum D_{max} . To make the calculations more precise the diode is forward voltage drop V_D is added [24]:

$$n = \frac{V_{in} \times D_{max}}{(1 - D_{max}) \times (V_{out} + V_D)} \quad \text{Equation III-2}$$

Numerical application:

$$n = 1.90 \approx 2$$

III.2.2 MOSFET selection

The function of the power switch is to control the flow of energy from the input power source to the output voltage. In the Flyback configuration, the switch (denoted as Q1 figure II-2) connects the input to the primary winding when is closed, and disconnects the input from the primary when it is open. The switch must be able to handle the current flowing through the transformer and withstand the voltage difference between the input and the primary winding

when closed. Additionally, the switch needs to transition quickly from one state to another to avoid excessive power dissipation during the switching transition.

The next step is to select the suitable MOSFET for our application, we calculate the maximum voltage $V_{DS_{max}}$ and current flowing through the MOSFET (I_{pk}) [24] :

$$V_{DS_{max}} = V_{in} + \frac{D_{max} \times V_{in}}{1 - D_{max}} \quad \text{Equation III-3}$$

Numerical application:

$$V_{DS_{max}} = 48V$$

$$I_{pk} = \frac{P_{in}}{D_{max} \times V_{in}} + \frac{D_{max} \times V_{in}}{2 \times F \times L_p} \quad \text{Equation III-4}$$

Numerical application:

$$I_{pk} = 4A$$

Note that a 20% security margin has been added to the voltage. however the current should be at least twice the maximum output current to ensure the converter's safe operation ($V_{DS_{max}}=58V$, $I_{pk}=8A$).

III.2.3 Diode selection

When the power switch is OFF, the diode conducts and allows the current to flow through the inductance. The important criteria for diode selection are switching speed, breakdown voltage, current handling capability, and reverse voltage to minimize power dissipation. The breakdown voltage should be greater than the maximum difference between the input voltage and the output voltage, with a certain margin added to accommodate transient voltage spikes. The current rating should be at least twice the maximum output current value. This is because power and junction temperature limitations play a significant role in device selection.

In this step, the rectifier diodes are assessed, Calculate the maximum voltage that the diode can withstand [24] :

$$VD_{pk} = V_{out} + \frac{V_{in}}{ns1} \quad \text{Equation III-5}$$

Numerical application:

$$VD_{pk} \approx 34.5V, \quad VD_{pk} = 24.63V + 40\% \text{ safety margin}$$

By adding a 40% safety margin, the maximum reverse voltage is determined to be 34.5V

III.2.4 Snubber components selection

To calculate the snubber components values, we suppose that the snubber voltage V_{sn} is equal to two times of nV_{out} (with n: turn ratio).

$$V_{sn} = (12 \times 2 \times 2) = 48V$$

The leakage inductance L_k is estimated to be 2% of the primary inductance L_p

$$L_k = 0.02 \times 100 = 2\mu H$$

R_{sn} is given by the following equation [21]:

$$R_{sn} = \frac{V_{sn}^2}{\frac{1}{2} * Lk * I_{pk}^2 * \left(\frac{V_{sn}}{V_{sn} - nV_{out}} \right) * F} \quad \text{Equation III-6}$$

Numerical application:

$$R_{sn} = 2.35k\Omega$$

R_{sn} : snubber resistance.

The maximum ripple of the snubber capacitor voltage is 10% of V_{sn} and the snubber capacitance C_{sn} is obtained as follows [21]:

$$C_{sn} = \frac{V_{sn}}{\Delta V_{sn} \times R_{sn} \times F} \quad \text{Equation III-7}$$

Numerical application:

$$C_{sn} = 141 \text{ nf}$$

III.2.5 Used components

In this section we have to choose the perfect components basing on previous calculation. Note that the selection of this components is based on availability in laboratory.

Refer to section III.2.3 the chosen diode is STTH60L06W.

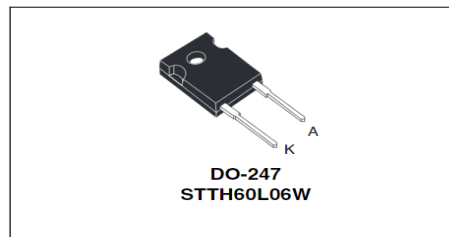


Figure III-1: STTH60L06W DIODE

The STTH60L06, which is using ST Turbo 2 600V technology, is especially suited for use in switching power supplies, and industrial applications, as rectification and discontinuous mode PFC boost diode. Thanks to its low V_f characteristics, this device exhibits high performances in free-wheeling applications.

Refer to section III.2.2 the chosen MOSFET is a high speed power switching transistor IRFP260M.

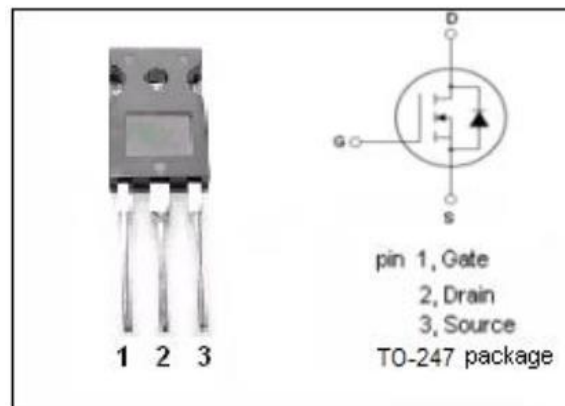


Figure III-2: IRFP260M Transistor

And finally for the snubber diode we followed the same steps for its selection and we have chosen RHRG75120 which is a Low loss, high performance and soft fast recovery diode used for switching power supplies.

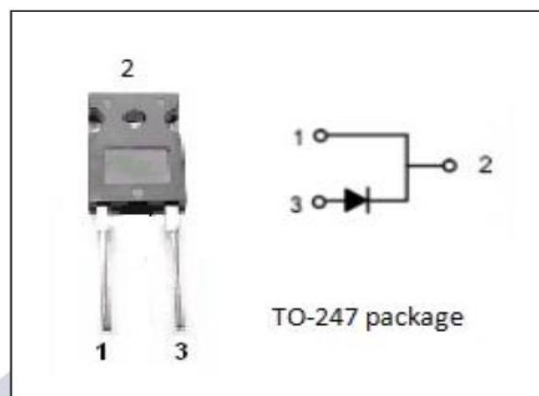


Figure III-3: RHRG75120 Diode

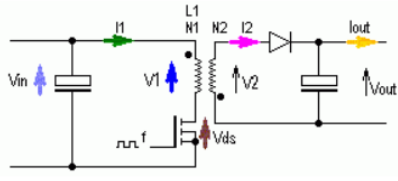
III.2.6 Core selection

Core selection is based on the frequency (30Khz) and the power working (24W) . The first step is to go to the magnetic ferrite core catalog [25] and searching for typical power handling chart table, then selecting the frequency and the power needed for our application. For more details, refer to the appendix. We found that the E25/13/7 core is the perfect core for our application. According to the availability in the laboratory we use ETD49 core, because E25/13/7 was not available. According to the magnetic ferrite core catalog ETD49 is also suitable for our converter.

To make sure of this selection, we tried another method to select the core, which is by resorting to the Schmidt walter web site [26]. The Schmidt walter web site is an online tool to design of switch mode power supplies and its transformers.

The Schmidt walter web site asks to enter the specification of the converter As shown in the following figure:

Fly-back Converter



| | | | |
|--|--|--|------------------|
| V_{in_min} / V | V_{in_max} / V | V_{in} / V for the calculations | |
| 20 | 30 | 24 | |
| V_{out} / V | I_{out} / A | f / kHz | Calculate |
| 12 | 2 | 30 | Transformer Data |
| <input checked="" type="checkbox"/> Proposal | L₁ / H : | 102.5E-6 | |
| <input checked="" type="checkbox"/> Proposal | N₁ / N₂ : | 1.97 | |

Figure III-4: The specification input values

By clicking on the button transformer data , a table appears presents suggestions of the suitable core begin from too small into very good core as shown in the following figure:

| No. | Core | Ident. | Manufacturer | A_L/nH | A_{in}/mm^2 | l_{in}/mm | A_{min}/mm^2 | $W_{max}/\mu Ws$ | B_{max}/mT | N1 | N2 |
|-----|-----------|--------|--------------|----------|---------------|-------------|----------------|------------------|--------------|----|----|
| 17 | ETD59 | 1.0 | Siemens | 508 | 368 | 139 | 368 | 11996 | 80 | 15 | 8 |
| 18 | ETD59 | 1.5 | Siemens | 381 | 368 | 139 | 368 | 15995 | 69 | 17 | 9 |
| 19 | ETD59 | 2.0 | Siemens | 311 | 368 | 139 | 368 | 19995 | 62 | 19 | 10 |
| 20 | E13/7/4 | 0.04 | Siemens | 250 | 12.4 | 29.6 | 12.2 | 27 | 1687 | 21 | 11 |
| 21 | E16/8/5 | 0.1 | Siemens | 242 | 20.1 | 37.6 | 19.4 | 80 | 377 | 22 | 12 |
| 22 | E16/8/5 | 0.5 | Siemens | 69 | 20.1 | 37.6 | 19.4 | 245 | 557 | 39 | 20 |
| 23 | E20/10/6 | 0.25 | Siemens | 162 | 32.1 | 46.3 | 31.9 | 283 | 519 | 26 | 14 |
| 24 | E20/10/6 | 0.5 | Siemens | 100 | 32.1 | 46.3 | 31.9 | 458 | 408 | 33 | 17 |
| 25 | E25/13/7 | 0.25 | Siemens | 250 | 52.5 | 57.5 | 51.5 | 477 | 400 | 21 | 11 |
| 26 | E25/13/7 | 0.5 | Siemens | 151 | 52.5 | 57.5 | 51.5 | 790 | 311 | 27 | 14 |
| 27 | E25/13/7 | 1.0 | Siemens | 91 | 52.5 | 57.5 | 51.5 | 1312 | 241 | 34 | 18 |
| 28 | E30/15/7 | 0.18 | Siemens | 300 | 60 | 67 | 49 | 360 | 460 | 19 | 10 |
| 29 | E30/15/7 | 0.34 | Siemens | 195 | 60 | 67 | 49 | 554 | 371 | 23 | 12 |
| 30 | E32/16/9 | 0.5 | Siemens | 244 | 83 | 74 | 81.4 | 1222 | 250 | 21 | 11 |
| 31 | E32/16/9 | 1.0 | Siemens | 145 | 83 | 74 | 81.4 | 2056 | 193 | 27 | 14 |
| 32 | E36/18/11 | 0.5 | Siemens | 312 | 120 | 81 | 112 | 1809 | 205 | 19 | 10 |
| 33 | E36/18/11 | 1.0 | Siemens | 183 | 120 | 81 | 112 | 3085 | 157 | 24 | 13 |
| 34 | E42/21/15 | 0.5 | Siemens | 454 | 178 | 97 | 175 | 3036 | 158 | 16 | 9 |
| 35 | E42/21/15 | 0.64 | Siemens | 378 | 178 | 97 | 175 | 3646 | 145 | 17 | 9 |
| 36 | E42/21/15 | 1.0 | Siemens | 272 | 178 | 97 | 175 | 5067 | 123 | 20 | 11 |
| 37 | E42/21/15 | 1.5 | Siemens | 201 | 178 | 97 | 175 | 6856 | 105 | 23 | 12 |
| 38 | E42/21/20 | 0.5 | Siemens | 603 | 234 | 97 | 229 | 3914 | 140 | 14 | 8 |

L=102.5μH

The core is...
very good
gut
 suitable
 too small

[Help](#)

[Print](#)

Wire Data:
 $d_1 \geq 0.66 \text{ mm}$
 $A_1 \geq 0.34 \text{ mm}^2$
 $d_2 \geq 1.13 \text{ mm}$
 $A_2 \geq 0.67 \text{ mm}^2$

[OK](#)

| Core | Ident. | Manufacturer | A_L/nH | A_{in}/mm^2 | l_{in}/mm | A_{min}/mm^2 |
|------|--------|--------------|----------|---------------|-------------|----------------|
| | | | | | | |

Add

Figure III-5: The table of proposals cores 1

In the previous table, the E25/13/7 core appears in green color, which means, it is very good for our application. Also the ETD49 core is suitable for our application as shown in the following figure:

| No. | Core | Ident. | Manufacturer | A_L/nH | A_{in}/mm^2 | l_{in}/mm | A_{min}/mm^2 | $W_{max}/\mu Ws$ | B_{max}/mT | N1 | N2 |
|-----|-------|--------|--------------|----------|---------------|-------------|----------------|------------------|--------------|----|----|
| 2 | ETD29 | 0.5 | Siemens | 201 | 76 | 70.4 | 71 | 1129 | 260 | 23 | 12 |
| 3 | ETD29 | 1.0 | Siemens | 124 | 76 | 70.4 | 71 | 1829 | 204 | 29 | 15 |
| 4 | ETD34 | 0.5 | Siemens | 251 | 97.1 | 78.6 | 91.6 | 1504 | 225 | 21 | 11 |
| 5 | ETD34 | 1.0 | Siemens | 153 | 97.1 | 78.6 | 91.6 | 2468 | 176 | 26 | 14 |
| 6 | ETD39 | 0.5 | Siemens | 326 | 125 | 92.2 | 123 | 2088 | 191 | 18 | 10 |
| 7 | ETD39 | 1.0 | Siemens | 196 | 125 | 92.2 | 123 | 3473 | 148 | 23 | 12 |
| 8 | ETD44 | 0.5 | Siemens | 438 | 173 | 103 | 172 | 3039 | 158 | 16 | 9 |
| 9 | ETD44 | 1.0 | Siemens | 262 | 173 | 103 | 172 | 5081 | 122 | 20 | 11 |
| 10 | ETD44 | 1.5 | Siemens | 194 | 173 | 103 | 172 | 6862 | 105 | 23 | 12 |
| 11 | ETD49 | 0.5 | Siemens | 525 | 211 | 114 | 209 | 3744 | 143 | 14 | 8 |
| 12 | ETD49 | 1.0 | Siemens | 314 | 211 | 114 | 209 | 6260 | 110 | 19 | 10 |

L=102.5μH

The core is...
very good
gut
 suitable
 too small

[Help](#)

[Print](#)

Figure III-6: Table of proposals cores 2

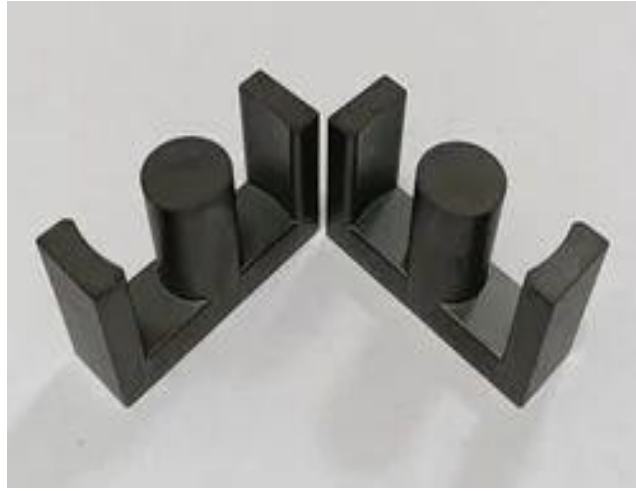


Figure III-7:ETD49 ferrite core

After the selection of the core we need to calculate the number of turns for each winding begin with the secondary winding N_s the number of turns is given by the following equation:

$$AL = \frac{LP}{N^2} \quad \text{Equation III-8}$$

$$N_s^2 = \frac{LP}{AL} \Leftrightarrow N = \sqrt{\frac{LP}{AL}} \quad \text{Equation III-9}$$

Numerical application :

$$N_s = \sqrt{\frac{100000}{314}} = 18 \text{ turns}$$

By having 18 turns in the secondary winding we calculate the primary winding N_p , basing on turn ratio n ($n=1.9$).

$$N_s = n * N_p \Leftrightarrow N_p = \frac{N_s}{n} \quad \text{Equation III-10}$$

Numerical application :

$$N_p = \frac{18}{1.9} = 9.4 \approx 10 \text{ turns}$$

III.3 Simulation

In the simulation part, we have used Pspice software, Pspice is a popular and widely used electronic circuit simulation software. We have chosen Pspice for the following reasons:

- It is based on the industry-standard SPICE and provides access to libraries of models developed by manufacturers.

- It allows for seamless integration of digital and analog components.
- The software is user-friendly and easy to use.
- It is a comprehensive tool that can simulate various aspects of power electronics systems, analog and digital control electronics, and feedback control systems.
- It provides results that closely approximate real-world outcomes.
- Model editor option, which allows us to create, edit, and manage component models, such as transistors, diodes, Nonlinear transformer and inductance, and other electronic devices, that are not readily available in the default PSPICE library.

For our simulation we have followed the following steps to make the transformer basing on the data of the ETD 49 from the ETD49 data sheet [27]

Open the Model Editor from Start/All Programs/Cadence/Release xy.z/ PSpice Accessories directory, the PSpice Model Editor pops up Select File/New, from the Model menu select New. On the New window, we write the name of Model Name (ETD49) and as model choose “Magnetic Core” as shown in the following figure:

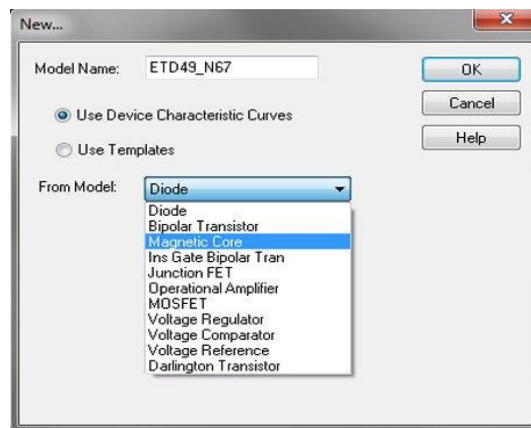


Figure III-8:choosing model window

After this The Hysteresis Curve window opens for this step we need to obtain the core's datasheet, which provides information about its characteristics, including the winding configuration, core material, and dimensions.

we can set two geometrical parameters for the support ETD49, reporting the AREA and PATH parameters from the datasheet.

| | | | | | | |
|------|------|--------|--------|-----|--|-------------------------------------|
| AREA | 2.11 | 1e-006 | 1e+030 | 0.1 | | <input checked="" type="checkbox"/> |
| PATH | 11.4 | 1e-006 | 1e+030 | 1 | | <input checked="" type="checkbox"/> |

Figure III-9:the PATH and the AREA parameters

From the ferrite datasheet we find a value of Initial permeability of 2100. Write this data in the edit field as shown in the following figure:

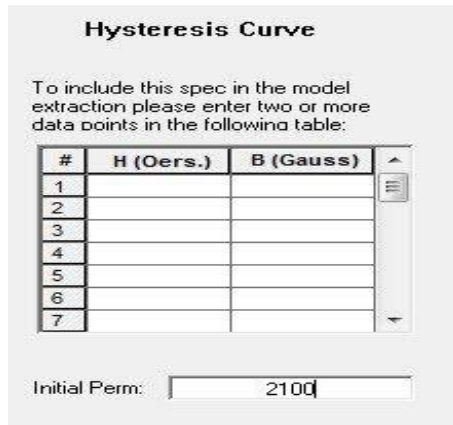


Figure III-10:hysteresis curve table

To fill this table, we need a set of points that we can get From the Epcos datasheet derive a graph useful for tracing the dynamic magnetization curve through couple of points B-H As shown in the following figure:

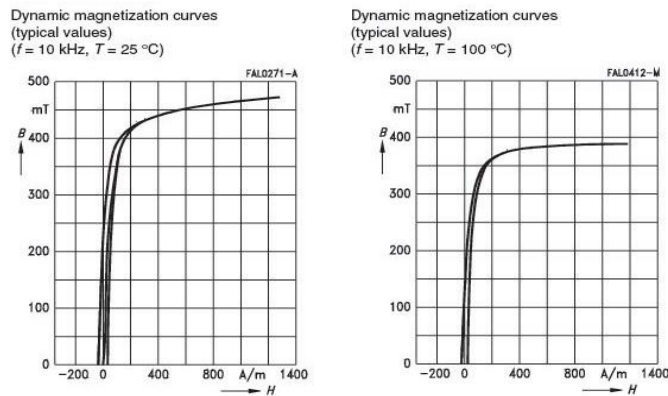


Figure III-11:Magnetic curves of the ETD49

After filling in the table, we obtain the following results:

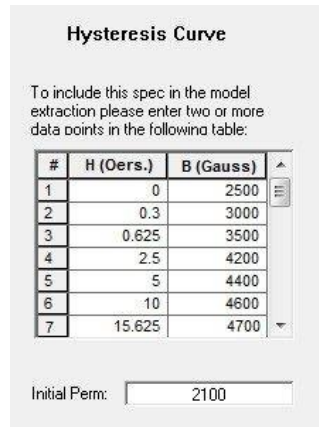


Figure III-12:the hystiresis filled table

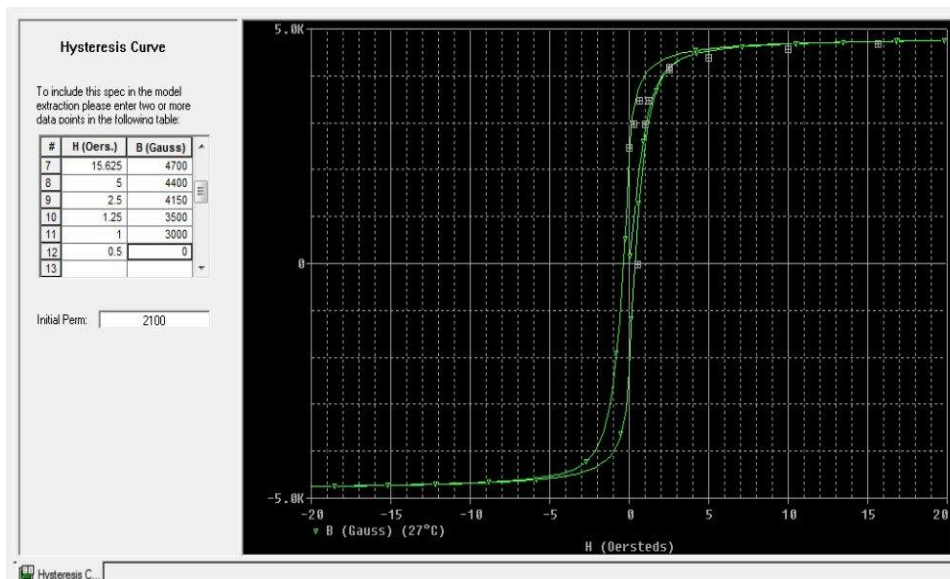


Figure III-13:The resultant Hysteresis curve

Now we open a new project and pickup the XFRM_NONLINEAR model from the BREAKOUT library:

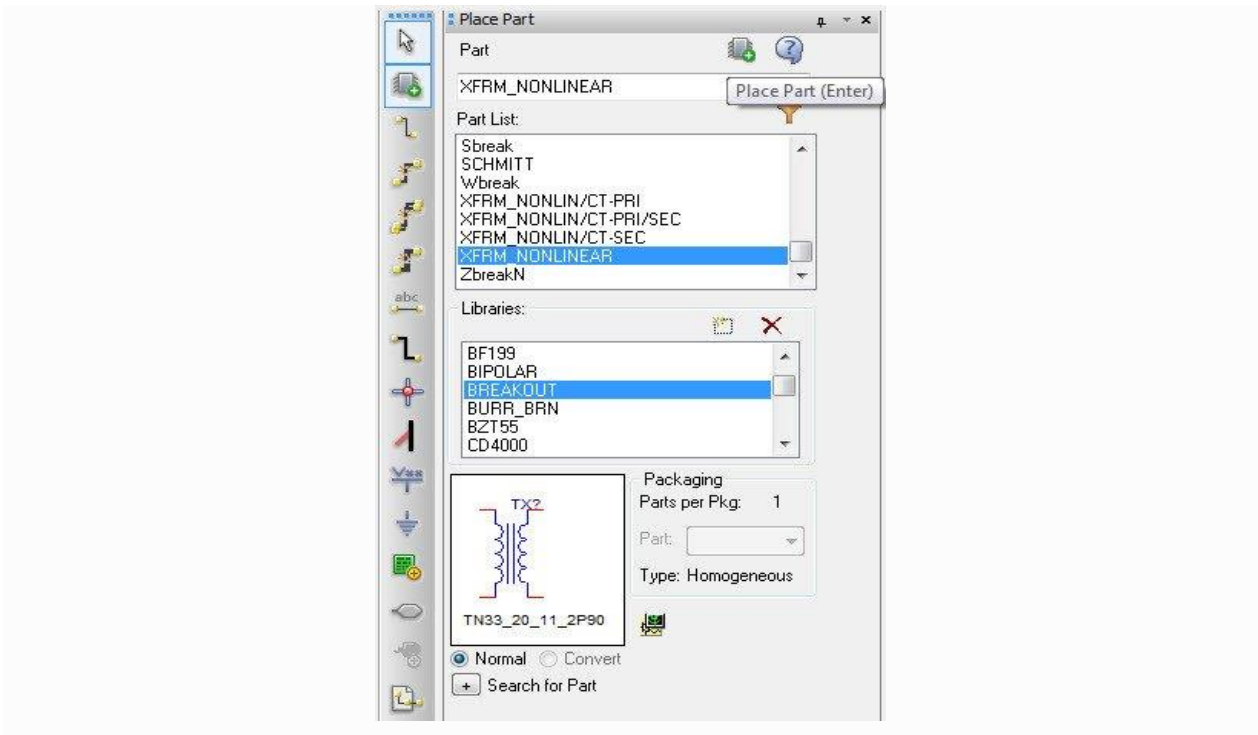


Figure III-14:Transformer selection

Place the component, select it, mouse dx button/Edit Properties. the property window pops up, write the name of implementation and the path to the library and Report the number of turns of primary and secondary, L1_TURNS=19 and L2_TURNS=10

| | |
|------------------------------|--------------------------|
| Designator | |
| Graphic | XFRM_NONLINEAR.Normal |
| ID | |
| Implementation | TN33_20_11_2P90 |
| Implementation Path | C:\Cadence\SPB_16.5\l... |
| Implementation Type | PSpice Model |
| L1_TURNS | 19 |
| L2_TURNS | 10 |
| Location X-Coordinate | 570 |
| Location Y-Coordinate | 80 |
| Name | INS14303 |
| Part Reference | TX1 |
| PCB Footprint | |
| Power Pins Visible | <input type="checkbox"/> |
| Primitive | DEFAULT |
| PSpiceOnly | TRUE |
| PSpiceTemplate | K*@REFDES L1*@REFDES |
| Reference | TX1 |
| Source Library | C:\CADENCE\SPB_16... |
| Source Package | XFRM_NONLINEAR |
| Source Part | XFRM_NONLINEAR.Norm |
| Value | ETD49_67 |

Figure III-15:properties of the transformer

After the enter of L_1 and L_2 , we Use the PSpice component library to find models for the power switch (MOSFET or IGBT), diode, capacitor. Then Assign appropriate values to the component

parameters based on our design requirements and specifications. The following figure represent our circuit design:

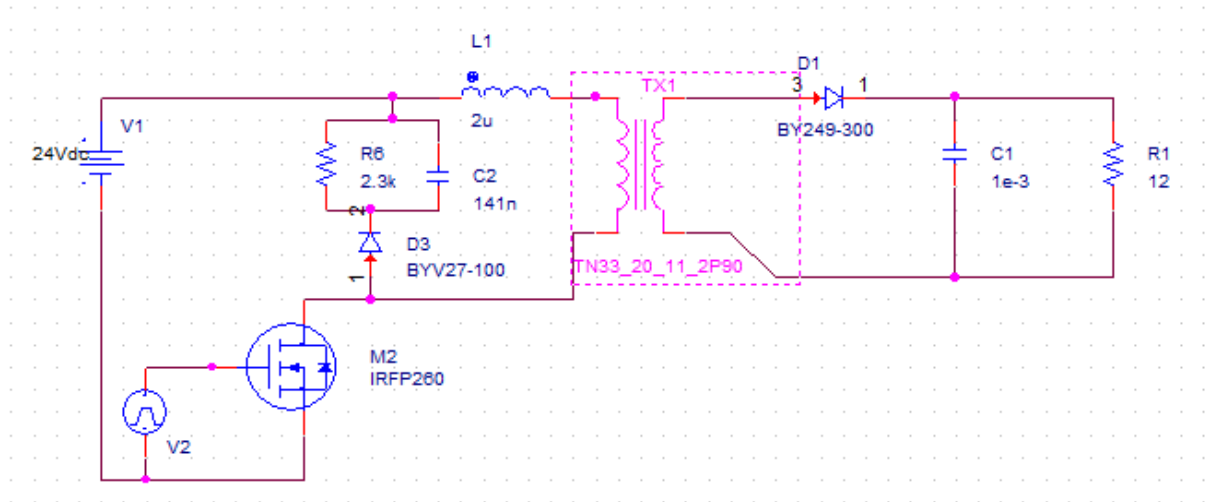


Figure III-16:flyback converter circuit

After selecting the components and drawing the circuit we run the simulation. the obtain results are present in the following figure :

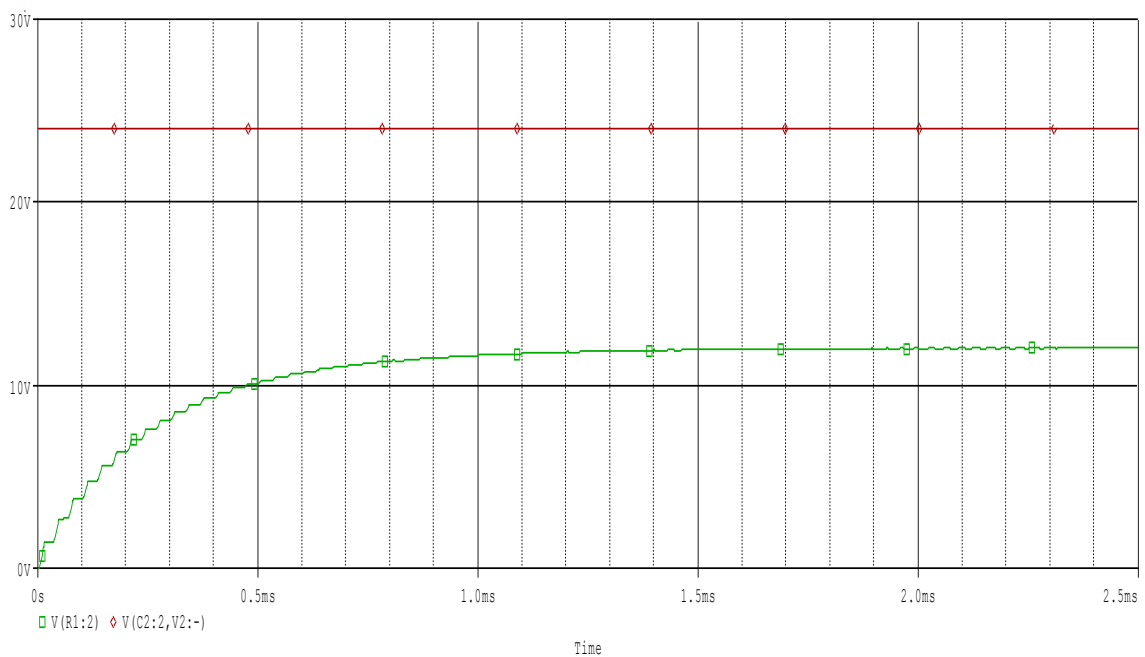


Figure III-17:the simulation results

The input voltage is represented by the red curve.

The output voltage is represented by the green curve.

Basing on this simulation results we remark that the output voltage is around 12 volts witch is the desired value even the input is 24 volts . Our converter works perfectly.

III.4 Experimental setup

The following figure represent the physical realization of the Flyback converter, meticulously assembled according to the design parameters derived from simulations and calculations. This experimental setup served as the foundation for practical testing and validation, enabling a seamless transition from theoretical design to real-world application.

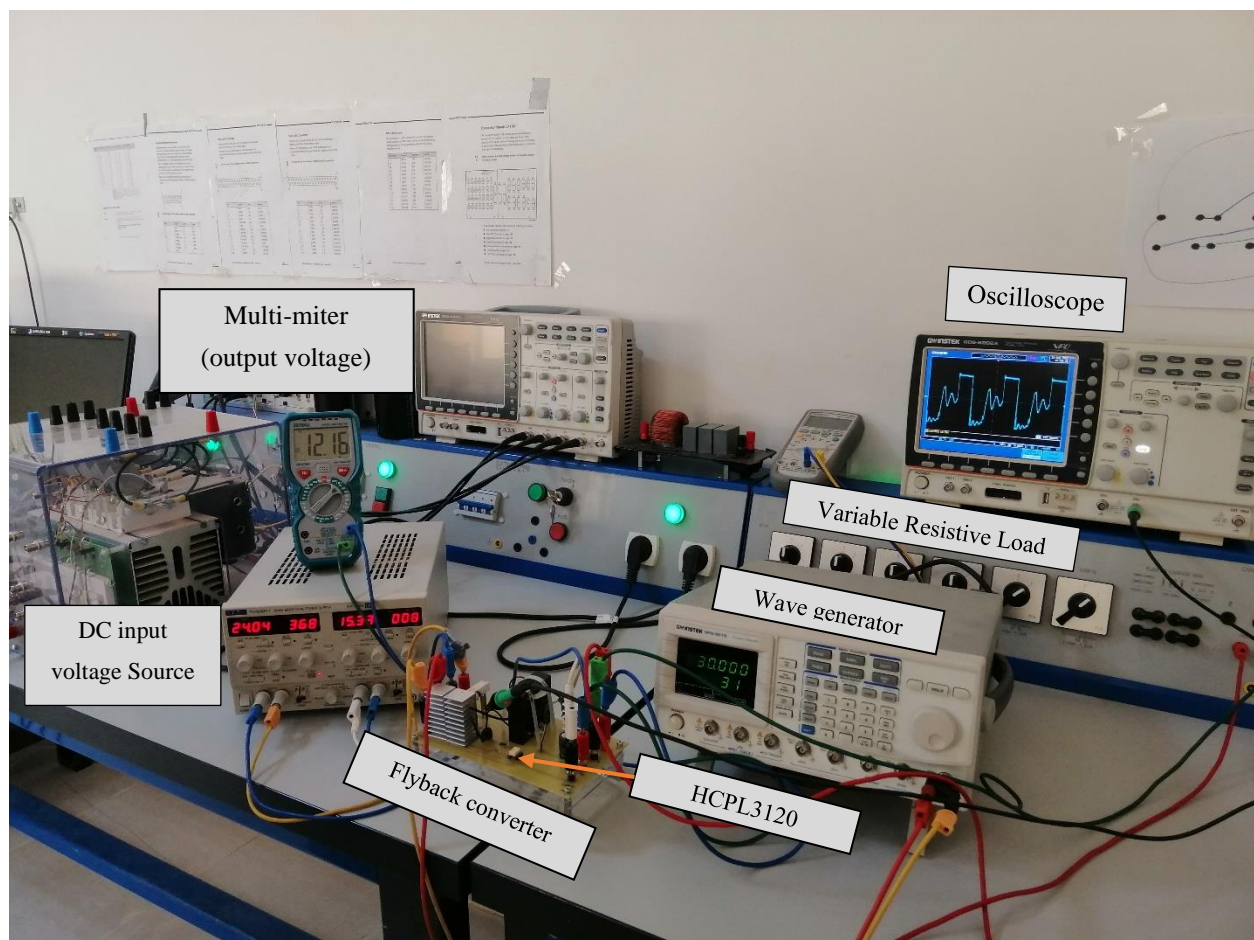


Figure III-18: real photo of realization

III.4.1 MOSFET driving circuit

The HCPL-3120 gate drive optocouplers contain a GaAsP LED. The LED is optically coupled to an integrated circuit with a power output stage. It is ideally suited for driving power IGBTs and MOSFETs used in motor controller inverted applications. The high operating voltage range of the output stage provides the drive voltages required by gate controlled devices.

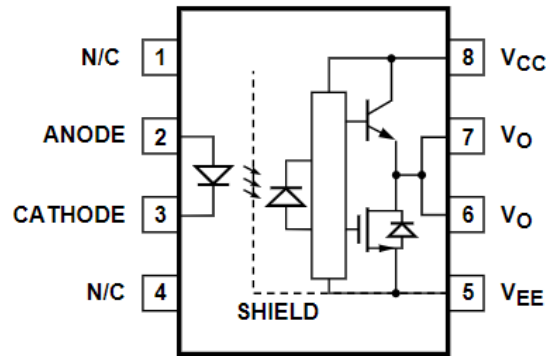


Figure III-19:Functional diagram of HCPL 3120

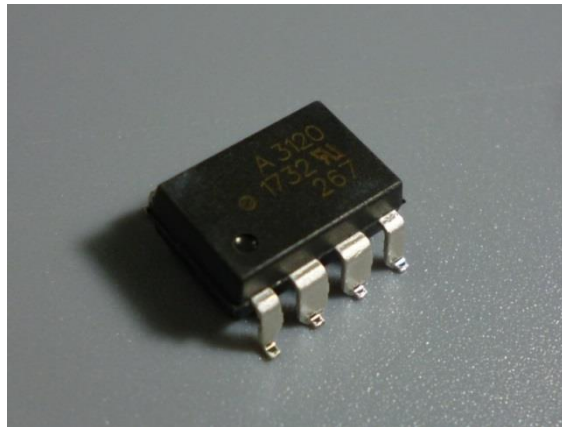


Figure III-20:HCPL 3120

In our converter, we have used HCPL3120 to benefit the optical isolation

III.4.2 The results achieved through the realization

After the selection of the components , we successfully designed the Flyback converter. To evaluate its performance, we use the realized converter in the two cases of implementation the first one is open-loop configurations and the second is the closed-loop configuration.

the realized circuit is presented in the following figure:

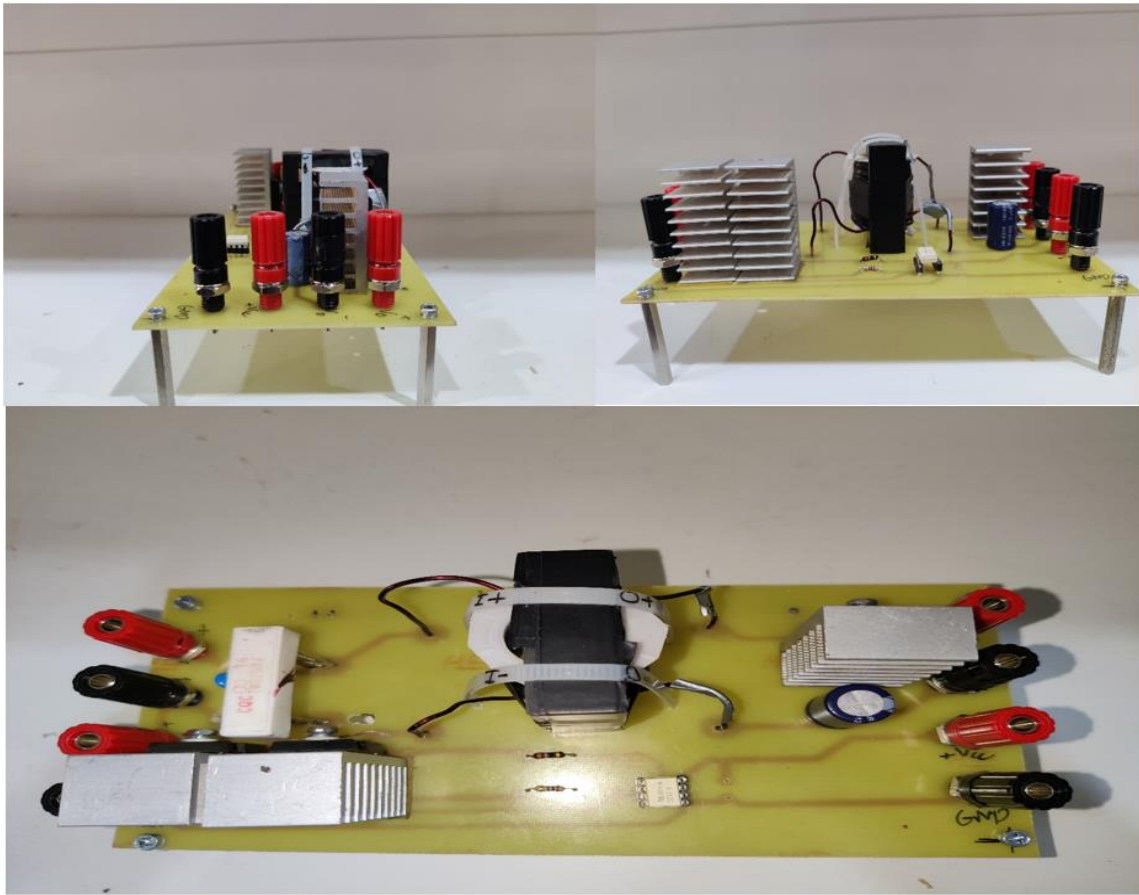


Figure III-21: the realized Flyback converter

III.4.2.1 Open loop implementation

The open-loop testing phase involved verifying the converter's behavior under basic operating conditions. For the PWM signal we use an external wave generator as presented in figure III-18.

The following figure represents the primary winding voltage:

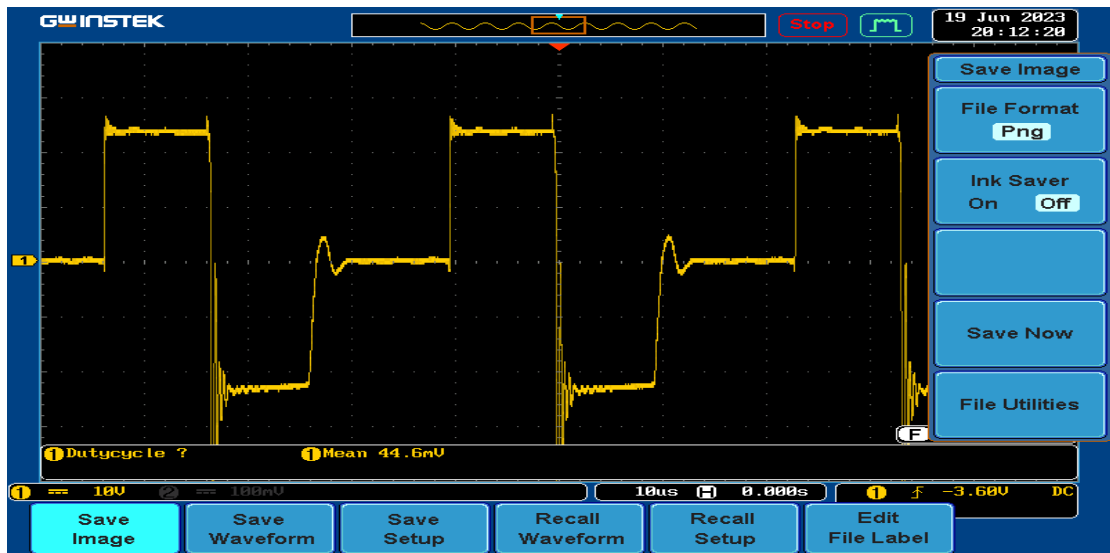


Figure III-22:primary winding voltage

The following figure represents the secondary winding voltage:

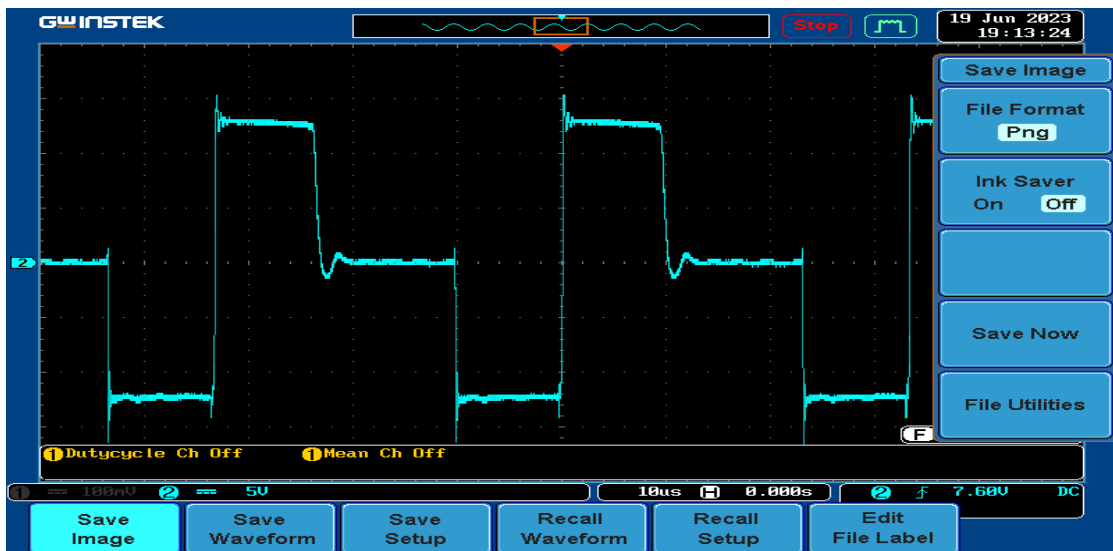


Figure III-23: secondary winding voltage

The following figure represents the primary winding current :



Figure III-24: Primary winding current

The following figure represents the secondary winding current:



Figure III-25: Secondary winding current

Comment: after reviewing the results obtained from our practical implementation, we found similar outcomes to those obtained in the theoretical aspect discussed in Chapter 2 in figure II.7 .

III.4.2.2 Closed loop implementation

Modelling of Flyback converter:

State space averaging approximates the switching converter as a continuous linear system. In state space average modelling, the switching circuit is split into two (Continuous Conduction Mode) or three (Discontinuous Conduction Mode) different structure. Base of modern control theory is the state-space modelling of dynamical systems. The state-space averaging method is

else identical to the technique of deriving the small-signal ac model. To derive the small-signal averaged calculations of the PWM switching converters we make use of this explanation of state-space averaging technique.

To make the calculation close to the reality we take consideration of the resistance of the MOSFET (R_{sw}) and capacitor (R_c) and the forward voltage as shown in the following figure:

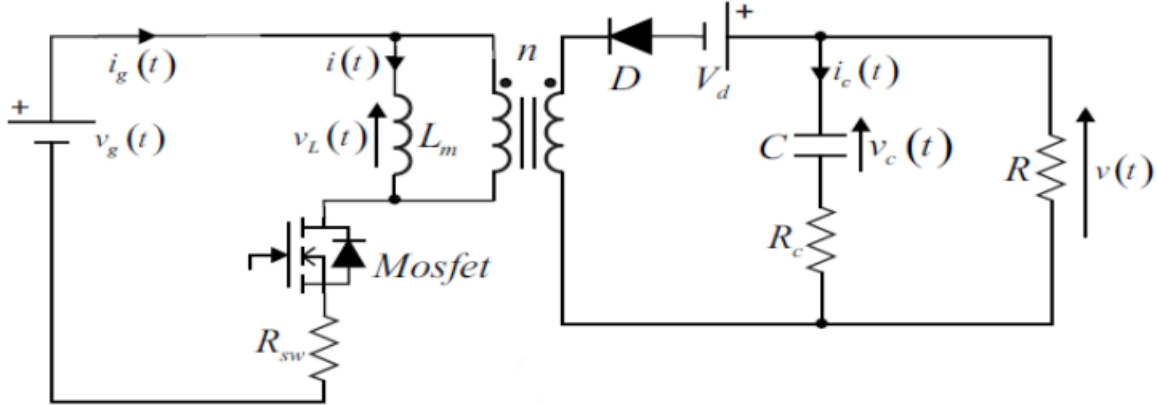


Figure III-26: based circuit of Flyback converter

To determine the transfer function of a flyback converter by considering its on and off times, several steps must be followed. Firstly, establish the converter's small-signal model, which involves linearizing its circuit equations around a steady-state operating point. Next, identify the on-time and off-time intervals of the switching cycle, as these represent distinct operating modes for the converter. In each mode, derive the small-signal equations that describe the converter's behavior, taking into account the variations in voltage and current. Then, using these equations, apply control theory techniques, such as state-space analysis or Laplace transforms, to formulate the overall transfer function that relates the converter's input to its output. This transfer function encapsulates the dynamic response of the flyback converter and is crucial for designing and analyzing its control system.

When the switch is on we have:

$$V_L = V_g - R_{sw} i_g \tag{Equation III-11}$$

$$i_c = \frac{-V_c}{R + R_c} \tag{Equation III-12}$$

$$i_g = i \quad \text{Equation III-13}$$

$$V = \frac{V_c R}{R + R_c} \quad \text{Equation III-14}$$

When the switch is off:

$$VL = (V_c - i_c R_c - V_d)n \quad \text{Equation III-15}$$

$$i_c = -(in + \frac{V}{R}) \quad \text{Equation III-16}$$

$$i_g = 0 \quad \text{Equation III-17}$$

$$V = V_c - i_c R_c \quad \text{Equation III-18}$$

The average inductor voltage can be expressed by combining the equations obtained during the two periods ON and OFF:

$$\langle V_L \rangle = V_g d1 - R_{sw} i_g d1 + V_c n d2 - i_c R_c n d2 - V_d n d2 \quad \text{Equation III-19}$$

This primes to the subsequent calculation for the average inductor current

$$L \frac{di}{dt} = V_g d1 - R_{sw} i_c d1 + V_c n d2 - i_c R_c n d2 - V_d n d2 \quad \text{Equation III-20}$$

The average capacitor current now can be initiated by averaging the subintervals concluded over one switching period, which fallouts to be

$$\langle i_c \rangle = \frac{-V_c}{R + R_c} d1 - ind2 - \frac{V}{R} d2 \quad \text{Equation III-21}$$

This primes to the subsequent calculation for the average capacitor voltage

$$\frac{Cdv_c}{dt} = \frac{-V_c}{R + R_c} d1 - Ind2 - \frac{V}{R} d2 \quad \text{Equation III-22}$$

The converter output voltage now can be expressed by averaging subintervals over one switching period:

$$\langle V \rangle = \frac{V_c R}{R + R_c} d1 + V_c d2 - i_c R_c d2 \quad \text{Equation III-23}$$

The input current of the converter can now be expressed by averaging the subintervals over one switching period, resulting

$$i_g = id1 + 0 \quad \text{Equation III-24}$$

Equations (III.20), (III.22), (III.23), and (III.24) are nonlinear differential equations involving duty cycles $d1(t)$ and $d2(t)$. Linearizing them yields a small-signal AC model where converter duty cycles and input voltage can be expressed as steady-state values with minor AC fluctuations.

$$d1 = D1 + \widehat{d1} \quad \text{Equation III-25}$$

$$i = I + \widehat{i} \quad \text{Equation III-26}$$

$$V_c = V_c + \widehat{v_c} \quad \text{Equation III-27}$$

$$V = V + \widehat{v} \quad \text{Equation III-28}$$

$$V_g = V_g + \widehat{v_g} \quad \text{Equation III-29}$$

$$i_c = I_c + \widehat{i_c} \quad \text{Equation III-30}$$

$$i_g = I_g + \hat{i}_g$$

Equation III-31

the large-signal averaged inductor (III.20) converts to with these substitution is expressed below,

$$L \frac{d(I+i)}{dt} = (V_g + \widehat{v}_g)(D1 + \widehat{d1}) - R_{sw}(I_g + \hat{i}_g)(D1 + \widehat{d1}) + (V_c + \widehat{v}_c)n(D2 + \widehat{d1})(I_c + \hat{i}_c)R_c n(D2 + \widehat{d1}) - V_d n(D2 + \widehat{d1})$$

Equation III-32

After simplification, we find:

$$L \left(\frac{d(I)}{dt} + \frac{d\hat{i}}{dt} \right) = (V_g D1 - R_{sw} I_g D1 + V_c n D2 - I_c R_c n D2 - V_d n D2) + (V_g \widehat{d1} + \widehat{v}_g D1 - R_{sw} I_g \widehat{d1} - R_{sw} \hat{i}_g D1 - V_c n \widehat{d1} + \widehat{v}_c n D2 + I_c R_c n \widehat{d1} - \hat{i}_c R_c n D2 + V_d n \widehat{d1}) + (\widehat{v}_g \widehat{d1} - R_{sw} \hat{i}_g \widehat{d1} - \widehat{v}_c n \widehat{d1} + \hat{i}_c R_c n \widehat{d1} + V_d \widehat{d1})$$

Equation III-33

The equation has three term types: DC (constant), first-order AC (linear response to AC variations), and second-order AC (product of variations). Assumed: AC variations are minor compared to DC value

$$\left\{ \begin{array}{l} |\widehat{v}_g| \ll |V_g| \\ |\widehat{d1}| \ll |D1| \\ |\hat{i}_g| \ll |I_g| \\ |\hat{i}| \ll |I| \\ |\widehat{v}_c| \ll |V_c| \\ |\hat{v}| \ll |V| \\ |\hat{i}_c| \ll |I_c| \end{array} \right.$$

Equation III-34

Meeting the small signal estimate (III.34) renders the second-order terms negligible compared to the dominant first-order terms, underscoring the importance of focusing on the DC terms.

$$V_g D1 - R_{sw} I_g D1 + V_c n D2 - I_c n R_c D2 - V_d n D2 = 0$$

Equation III-35

The first order terms essentially follow:

$$\frac{L d\hat{i}}{dt} = V_g \widehat{d1} + \widehat{v}_g D1 - R_{sw} I_g \widehat{d1} - R_{sw} \hat{i}_g D1 - V_c n \widehat{d1} + \widehat{v}_c n D2 + I_c R_c n \widehat{d1} - \hat{i}_c R_c n D2 + V_d n \widehat{d1}$$

Equation III-36

This equation is a linear expression that describes ac dissimilarities in the inductor current

On substituting equations (III.25)-(III.31) into (III.22), we obtain

$$\frac{Cd(V_c + \widehat{v}_c)}{dt} = \frac{-(V_c + \widehat{v}_c)}{R + R_c}(D1 + \widehat{d1}) - (I + \widehat{i})n(D2 - \widehat{d1}) - \frac{V + \widehat{v}}{R}(D2 - \widehat{d1}) \quad \text{Equation III-37}$$

Simplifying and sorting the above equation (III.37), we find

$$C \left(\frac{dV_c}{dt} + \frac{d\widehat{v}_c}{dt} \right) = \left(-\frac{V_c D1}{R + R_c} - InD2 - \frac{VD2}{R} \right) + \left(-\frac{V_c \widehat{d1}}{R + R_c} - \frac{\widehat{v}_c D1}{R + R_c} + In\widehat{d1} - \widehat{i}nD2 + \frac{V\widehat{d1}}{R} - \frac{\widehat{v}D2}{R} \right) + \left(-\frac{\widehat{v}_c \widehat{d1}}{R + R_c} + \widehat{i}n\widehat{d1} + \frac{\widehat{v}\widehat{d1}}{R} \right) \quad \text{Equation III-38}$$

Excluding second-order terms in equation (III.38), the focus remains on ensuring compliance with its DC terms.

$$-\frac{V_c D1}{R + R_c} - InD2 - \frac{VD2}{R} = 0 \quad \text{Equation III-39}$$

The first-order ac terms of (III.38) lead to the following small-signal for the ac capacitor voltage

$$\frac{Cd\widehat{v}_c}{dt} = -\frac{V_c \widehat{d1}}{R + R_c} - \frac{\widehat{v}_c D1}{R + R_c} + In\widehat{d1} - \widehat{i}nD2 + \frac{V\widehat{d1}}{R} - \frac{\widehat{v}D2}{R} \quad \text{Equation III-40}$$

Substitution of (III.25) -(III.31) into (III.23) leads to:

$$V + \widehat{v} = \frac{V_c + \widehat{v}_c}{R + R_c}R(D1 + \widehat{d1}) + (V_c + \widehat{v}_c)(D2 - \widehat{d1}) - (I_c + \widehat{i}_c)R_c(D2 - \widehat{d1}) \quad \text{Equation III-41}$$

On multiplying and sorting this equation, we obtain:

$$V + \widehat{v} = \left(\frac{V_c D1 R}{R + R_c} + V_c D2 - I_c R_c D2 \right) + \left(\frac{V_c R \widehat{d1}}{R + R_c} + \frac{R D1}{R + R_c} - V_c \widehat{d1} + \widehat{v}_c D2 + I_c R_c \widehat{d1} - \widehat{i}_c R_c D2 \right) + \left(\frac{\widehat{v}_c R \widehat{d1}}{R + R_c} - \widehat{v}_c \widehat{d1} + \widehat{i}_c R_c \widehat{d1} \right) \quad \text{Equation III-42}$$

The dc term must satisfy

$$V = \frac{V_c D1 R}{R + R_c} + V_c D2 - I_c R_c D2 \quad \text{Equation III-43}$$

the second-order terms in equation (III.42) is excluded and parting the following linearized ac expression:

$$\widehat{v} = \frac{V_c R \widehat{d1}}{R + R_c} + \frac{R D1}{R + R_c} - V_c \widehat{d1} + \widehat{v}_c D2 + I_c R_c \widehat{d1} - \widehat{i}_c R_c D2 \quad \text{Equation III-44}$$

Substituting equations (III.25)-(III.31) into (III.24) leads to

$$I_g + \hat{i}_g = (I + \hat{i})(D1 + \widehat{d1}) = (ID1) + (I\widehat{d1}) + (D1\hat{i}) + (\hat{i}\widehat{d1}) \quad \text{Equation III-45}$$

DC term must satisfy

$$I_g = ID1 \quad \text{Equation III-46}$$

By excluding second-order terms in equation (III.45), we simplify the following linearized AC expression.

$$\hat{i}_g = I\widehat{d1} + D1\hat{i} \quad \text{Equation III-47}$$

The equations of the quiescent values, (III.36), (III.40), (III.43), and (III.47) are collected below as

$$\begin{aligned} V_g d1 - R_{sw} i_c d1 + V_c n d2 - i_c R_c n d2 - V_d n d2 &= 0 \\ -\frac{V_c D1}{R + R_c} - I n D2 - \frac{V D2}{R} &= 0 \\ V &= \frac{V_c D1 R}{R + R_c} + V_c D2 - I_c R_c D2 \\ I_g &= ID1 \end{aligned} \quad \text{Equation III-48}$$

Assuming steady-state values for Vd, Vg, and D1, system (III.48) estimates I, Ig, V, Ic, and Vc. With five variables and four equations, a fifth equation is needed.

$$V = V_c - I_c R_c \quad \text{Equation III-49}$$

The outcomes of the expression are then introduced into the small-signal ac model

The small signal ac model, (III.36), (III.40), (III.44), and (III.47), is summarized below

$$\begin{aligned} \frac{L d\hat{i}}{dt} &= V_g \widehat{d1} + \widehat{v} g D1 - R_{sw} I_g \widehat{d1} - R_{sw} \hat{i}_g D1 - V_c n \widehat{d1} + \widehat{v} c n D2 + I_c R_c n \widehat{d1} \\ &\quad - \widehat{i} c R_c n D2 + V_d n \widehat{d1} \\ \frac{C d\widehat{v}c}{dt} &= -\frac{V_c \widehat{d1}}{R + R_c} - \frac{\widehat{v} c D1}{R + R_c} + I n \widehat{d1} - \widehat{i} n D2 + \frac{V \widehat{d1}}{R} - \frac{\widehat{v} D2}{R} \\ \widehat{v} &= \frac{V_c R \widehat{d1}}{R + R_c} + \frac{R D1}{R + R_c} - V_c \widehat{d1} + \widehat{v} c D2 + I_c R_c \widehat{d1} - \widehat{i} c R_c D2 \\ \hat{i}_g &= I \widehat{d1} + D1 \hat{i} \end{aligned} \quad \text{Equation III-50}$$

the state-space averaging technique to the second order Flyback converter. The autonomous state variables normally are the capacitor voltage $v_c(t)$ and the inductor current $i(t)$ which makes the state vector.

The voltage $v_g(t)$, and the voltage across the diode drop is an independent source V_d , which should be located in the input vector.

In order to design the converter input and output port, we want to find the input current $i_g(t)$ and output voltage $v(t)$ of the converter. In order to estimate this dependent current and voltage, it must be involved in the output vector $y(t)$.

When the MOSFET is conducting and the diode is off, we have :

$$\frac{CdV_c}{dt} = -\frac{V_c}{R + R_c} \quad \text{Equation III-51}$$

$$\frac{Ldi}{dt} = V_g - R_{sw}i \quad \text{Equation III-52}$$

$$i_g = i \quad \text{Equation III-53}$$

$$V = \frac{V_c R}{R + R_c} \quad \text{Equation III-54}$$

After organizing the terms, the result can be expressed in the subsequent state-space format:

$$\begin{bmatrix} \frac{di}{dt} \\ \frac{dV_c}{dt} \end{bmatrix} = \begin{bmatrix} -\frac{R_{sw}}{L} & 0 \\ 0 & -\frac{1}{RC + R_c C} \end{bmatrix} \begin{bmatrix} i \\ V_c \end{bmatrix} + \begin{bmatrix} \frac{1}{L} & 0 \\ 0 & 0 \end{bmatrix} \begin{bmatrix} V_g \\ V_d \end{bmatrix}$$

$$\begin{bmatrix} i_g \\ V \end{bmatrix} = \begin{bmatrix} 1 & 0 \\ 0 & \frac{R}{R + R_c} \end{bmatrix} \begin{bmatrix} i \\ V_c \end{bmatrix} + \begin{bmatrix} 0 & 0 \\ 0 & 0 \end{bmatrix} \begin{bmatrix} V_g \\ V_d \end{bmatrix}$$

When MOSFET is not conducting and diode is on:

$$i_g = 0 \quad \text{Equation III-55}$$

$$\frac{CdV_c}{dt} = -\frac{inR}{R-R_c} - \frac{V_c}{R-R_c} \quad \text{Equation III-56}$$

$$V = \frac{inR_cR}{R-R_c} + \frac{V_cR}{R-R_c} \quad \text{Equation III-57}$$

$$\frac{Ldi}{dt} = \frac{in^2R_cR}{R-R_c} + \frac{V_cnR}{R-R_c} - V_d n \quad \text{Equation III-58}$$

After the organization we obtain:

$$\begin{bmatrix} \frac{di}{dt} \\ \frac{dV_c}{dt} \end{bmatrix} = \begin{bmatrix} \frac{n^2R_cR}{LR-LR_c} & \frac{nR}{LR-LR_c} \\ -\frac{nR}{RC-R_cC} & -\frac{1}{RC-R_cC} \end{bmatrix} \begin{bmatrix} i \\ V_c \end{bmatrix} + \begin{bmatrix} 0 & -\frac{n}{L} \\ 0 & 0 \end{bmatrix} \begin{bmatrix} V_g \\ V_d \end{bmatrix}$$

$$\begin{bmatrix} i_g \\ V \end{bmatrix} = \begin{bmatrix} 0 & 0 \\ \frac{nR_cR}{R-R_c} & \frac{0}{R-R_c} \end{bmatrix} \begin{bmatrix} i \\ V_c \end{bmatrix} + \begin{bmatrix} 0 & 0 \\ 0 & 0 \end{bmatrix} \begin{bmatrix} V_g \\ V_d \end{bmatrix}$$

The next step is to combine the result and obtain the state-space averaged model as

$$A = A1D1 + A2D2 = \begin{bmatrix} -\frac{R_{sw}}{L} & 0 \\ 0 & -\frac{1}{RC+R_cC} \end{bmatrix} D1 + \begin{bmatrix} \frac{n^2R_cR}{LR-LR_c} & \frac{nR}{LR-LR_c} \\ -\frac{nR}{RC-R_cC} & -\frac{1}{RC-R_cC} \end{bmatrix} D2$$

$$A = \begin{bmatrix} -\frac{R_{sw}D1}{L} + \frac{n^2R_cRD2}{LR-LR_c} & \frac{nRD2}{LR-LR_c} \\ -\frac{nR}{RC-R_cC} & -\frac{D1}{RC+R_cC} - \frac{D2}{RC+R_cC} \end{bmatrix}$$

$$B = B1D1 + B2D2 = \begin{bmatrix} \frac{1}{L} & 0 \\ 0 & 0 \end{bmatrix} D1 + \begin{bmatrix} 0 & -\frac{n}{L} \\ 0 & 0 \end{bmatrix} D2 = \begin{bmatrix} \frac{D1}{L} & -\frac{nD2}{L} \\ 0 & 0 \end{bmatrix}$$

$$\begin{aligned}
C &= C1D1 + C2D2 = \begin{bmatrix} 1 & 0 \\ 0 & \frac{R}{R + R_c} \end{bmatrix} D1 + \begin{bmatrix} 0 & 0 \\ \frac{nR_c R}{R - R_c} & \frac{R}{R - R_c} \end{bmatrix} D2 \\
&= \begin{bmatrix} D1 & 0 \\ \frac{nR_c R D2}{R - R_c} & \frac{R D1}{R + R_c} + \frac{R D2}{R + R_c} \end{bmatrix} \\
E &= E1D1 + E2D2 = \begin{bmatrix} 0 & 0 \\ 0 & 0 \end{bmatrix} D1 + \begin{bmatrix} 0 & 0 \\ 0 & 0 \end{bmatrix} D2 = \begin{bmatrix} 0 & 0 \\ 0 & 0 \end{bmatrix}
\end{aligned}$$

Consequently, the required state-space averaged model of the flyback converter with basic parasitics:

$$\begin{aligned}
\begin{bmatrix} \frac{di(t)}{dt} \\ \frac{dVc(t)}{dt} \end{bmatrix} &= \begin{bmatrix} \frac{-R_{sw}D1}{L} + \frac{n^2 R_c R D2}{R L - R_c L} & \frac{n R D2}{R L - R_c L} \\ \frac{n R D2}{R C - R_c C} & -\frac{D1}{R C + R_c C} - \frac{D2}{R C - R_c C} \end{bmatrix} \begin{bmatrix} i(t) \\ vc(t) \end{bmatrix} \\
&+ \begin{bmatrix} \frac{D1}{L} & -\frac{n D2}{L} \\ 0 & 0 \end{bmatrix} \begin{bmatrix} Vg(t) \\ Vd \end{bmatrix} \\
\begin{bmatrix} ig \\ v(t) \end{bmatrix} &= \begin{bmatrix} D1 & 0 \\ \frac{n R_c R D2}{R - R_c} & \frac{R D1}{R + R_c} + \frac{R D2}{R - R_c} \end{bmatrix} \begin{bmatrix} i(t) \\ vc(t) \end{bmatrix} + \begin{bmatrix} 0 & 0 \\ 0 & 0 \end{bmatrix} \begin{bmatrix} Vg(t) \\ Vd \end{bmatrix}
\end{aligned}$$

For the closed loop implementation of our Flyback converter we used the dSPACE DS1103 which PPC Controller Board is specifically designed for development of high-speed multivariable digital controllers and real-time simulations in various fields. It is a complete real-time control system based on a PowerPC processor. For advanced I/O purposes, the board includes a slave-DSP subsystem based on the Texas Instruments TMS320F240 DSP microcontroller. The DS1103 PPC Controller Board is a standard PC/AT card that can be plugged into a PC using the ISA bus as a backplane. The card can also be inserted in a DSPACE expansion box communicating with the host PC via an ISA-bus extension or Ethernet.

Its For purposes of rapid control prototyping (RCP), specific interface connectors and connector panels provide easy access to all input and output signals of the board. Using an adapter cable, you can link your external signals from the 100-pin I/O connector on the board to Sub-D connectors. Therefore, you can make a high-density connection between the board and the devices of your application via Sub-D connectors.

It is fully programmable from the Simulink® block diagram environment and all I/O can be configured graphically. This is a quick and easy way to implement and test our control in a real environment.

The following figure represents the DS1103:



Figure III-27:dSPACE DS1103

The following figure represents the bloc diagram of a dSPACE Flyback converter with a PWM signal generation :

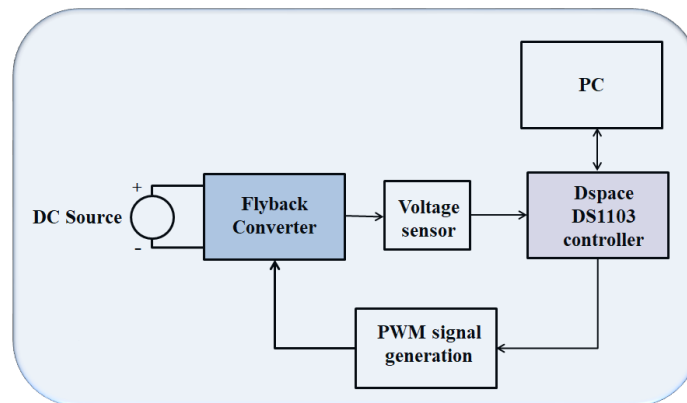


Figure III-28: dSPACE Flyback converter diagram

We will use a PID controller for the closed loop implementation in Dspace.

Most of the desired performance of a system can be achieved by suitable combination of Proportional, Integral and Derivative control action. The P-I-D controller is widely implemented because it is easy to understand and is quite operative. The transfer function of a PID controller is expressed by:

$$C(s) = k_p \left(1 + \tau_d s + \frac{1}{\tau_i s} \right)$$

It is a second order controller, but it has versatile applicability. Any type of SISO system can use this controller, e.g. linear, nonlinear, time delay, etc. For MIMO system, it is first decoupled into many SISO system and PID controller is implemented in each SISO system. Though, for suitable implementation, a controller has to be tuned for a precise process; i.e.

choice of P,I,D constraints are very important and process dependent. Unless the parameters are precisely selected, a controller may reason variability to the closed loop system.

The general variation with each controller parameter on a closed loop system is tabulated below:

Table III-1: The influence of the controller parameters

| Close loop response | Rise time | overshoot | Settling time | Steady state error |
|---------------------|--------------|-----------|---------------|--------------------|
| Kp | decrease | increase | Small change | decrease |
| Ki | decrease | increase | increase | decrease |
| Kd | Small change | decrease | decrease | no change |

Adjust each of the gains Kp, Ki and Kd until you obtain a desired overall response

It is not always essential that all the combination of proportional, derivative and integral actions should be combined in the controller. In our case, a simple P-I assembly will aid the objective.

In our Flyback converter, the feedback loop plays a crucial role in ensuring that the output voltage stays fixed at 12 volts no matter what changes happen to the input or the charge. The feedback loop constantly monitors the output voltage and adjusts the duty cycle of the converter's switching transistor to maintain the desired output voltage.

The primary components involved in the feedback loop of a Flyback converter are the optocoupler (typically an optoisolator) and a voltage reference. Here's how the feedback loop operates to regulate the output voltage:

First, the output voltage is monitored using a voltage divider network. The purpose is to create a feedback signal that accurately represents the output voltage level.

Secondly, The output voltage feedback signal is compared with a reference voltage inside the optocoupler which is 12 v. The optocoupler typically consists of an LED and a phototransistor. The LED is driven by the output voltage feedback signal, while the phototransistor is used to optically couple the feedback signal to the primary side of the converter.

Then the optocoupler phototransistor generates a proportional current based on the difference between the output voltage feedback signal and the reference voltage. This current is then amplified by an error amplifier circuit.

Thirdly ,The amplified error signal is fed into the pulse width modulation (PWM) controller of the flyback converter. The PWM controller adjusts the duty cycle of the switching

transistor according to the error signal. A higher duty cycle increases the energy transferred to the output, while a lower duty cycle reduces the energy.

The following figure represents the control of the flyback converter with simulink block:

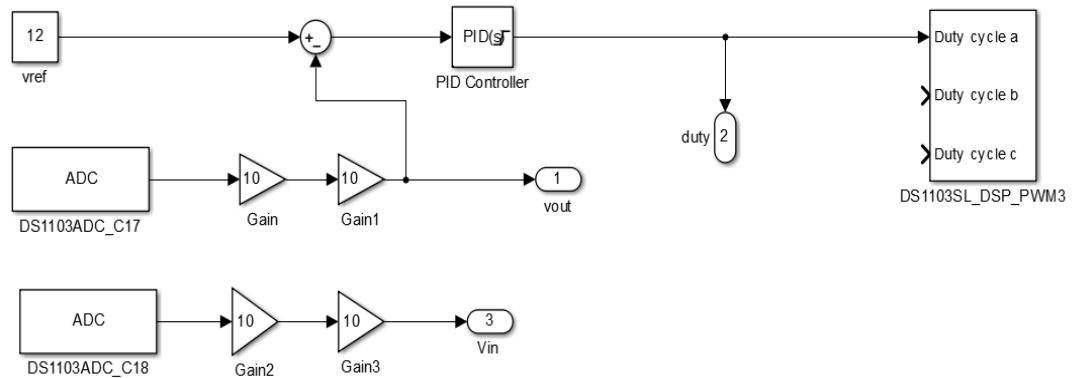


Figure III-29:Control of Flyback converter with simulink block

The output given by the voltage sensor is connected to channel ADC 17.

The input given by the voltage sensor is connected to channel ADC 18.

Vref: its our reference output.

III.4.3 Test of control

III.4.3.1 Results of test 1

Our primary objective in this closed-loop test is to assess the converter voltage regulation performance. By keeping the output voltage stable while intentionally altering the input voltage. we experimented with changing the input value between 20V to 27V and we obtain the following results:

The following figure represents the variation in our input voltage:

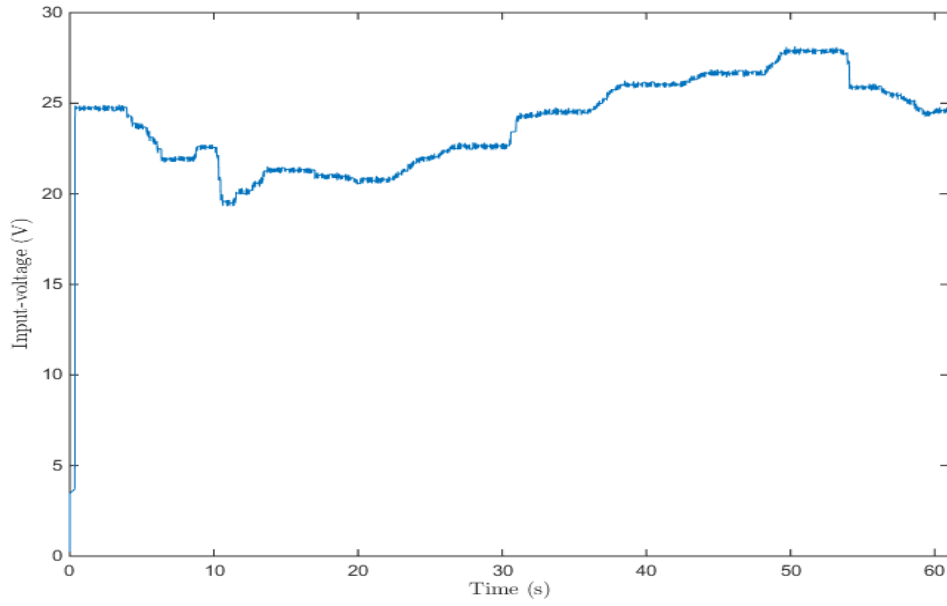


Figure III-30:Input voltage test 1

The following figure represents our output voltage:

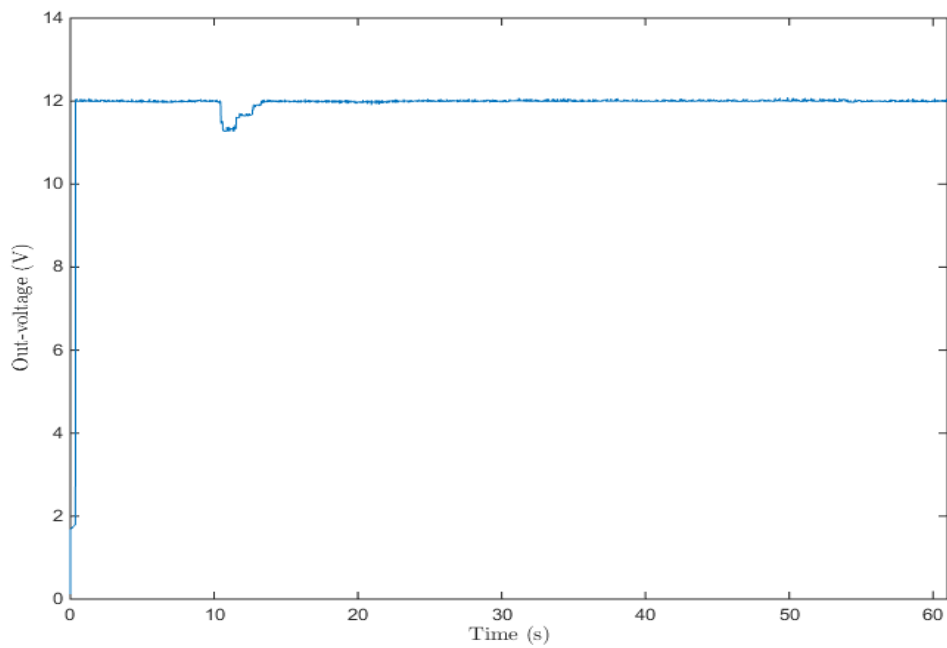


Figure III-31:Output voltage test 1

The following figure represents the duty cycle regulation:

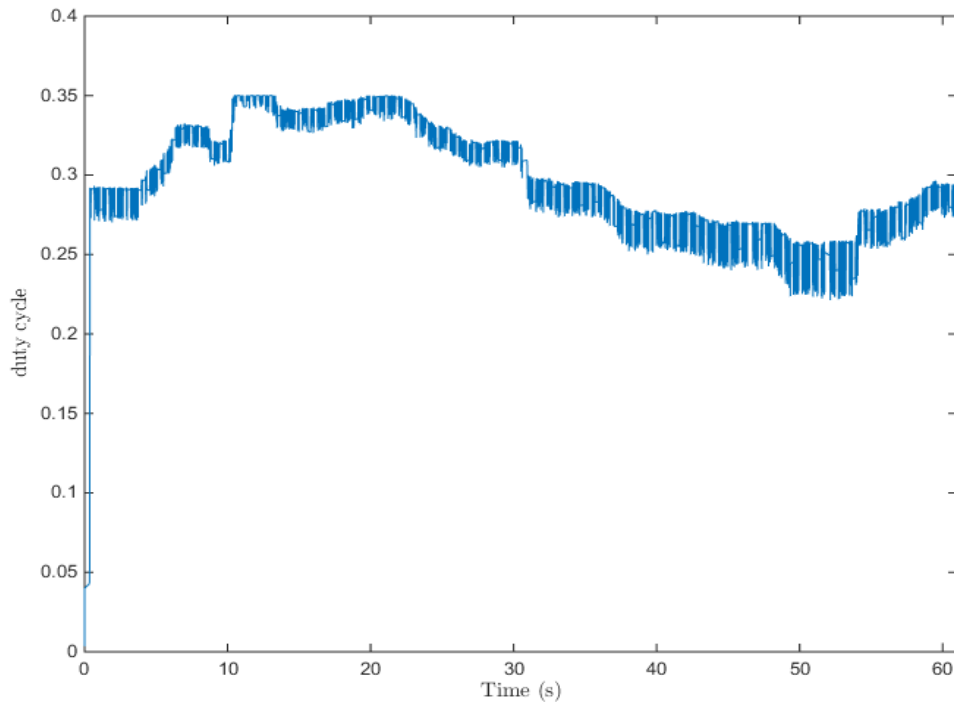


Figure III-32:Duty cycle test 1

After conducting the closed-loop testing phase, it is evident that our flyback converter has demonstrated exceptional voltage regulation capabilities. Across a range of input voltage levels, the output voltage remained remarkably stable, showcasing the effectiveness of our closed-loop control system.

we notice that the duty cycle changes by changing the input value in order to keep the output voltage around 12V, which means that our control is successfully working.

Note : we notice in the test that there has been a decline in the output curve, this is because we have fallen below the appropriate value for the transformer which is 20V to 30V.

III.4.3.2 Results of test 2

Our primary objective in this closed-loop test is to assess the converter voltage regulation performance. By keeping the output voltage stable while changing in the load value.

we experimented with changing the load value between 48Ω to 12Ω and we obtain the following results:

The following figure represents our input voltage:

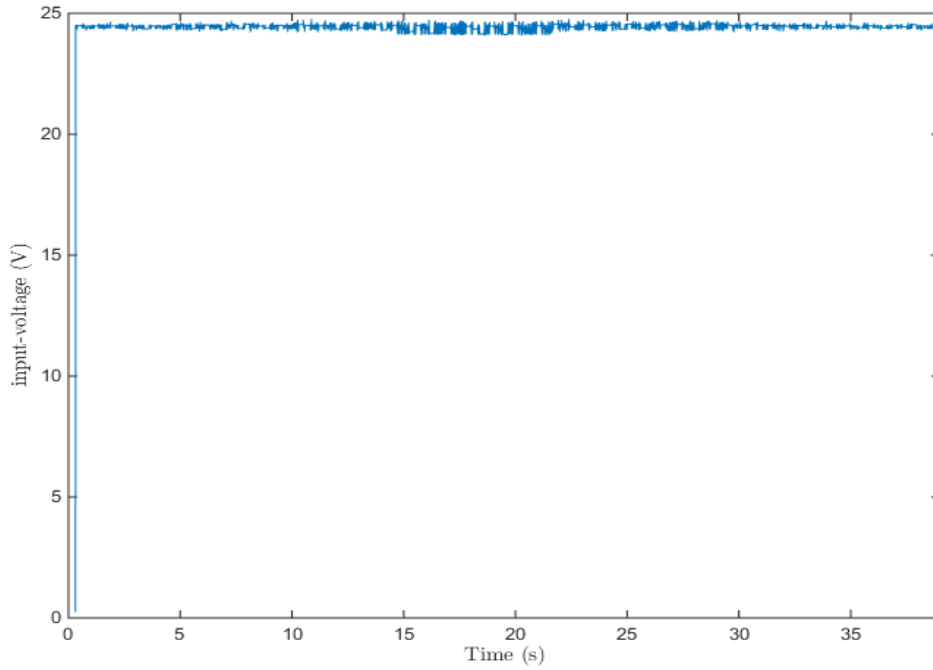


Figure III-33:Input voltage test 2

The following figure represents our output voltage:

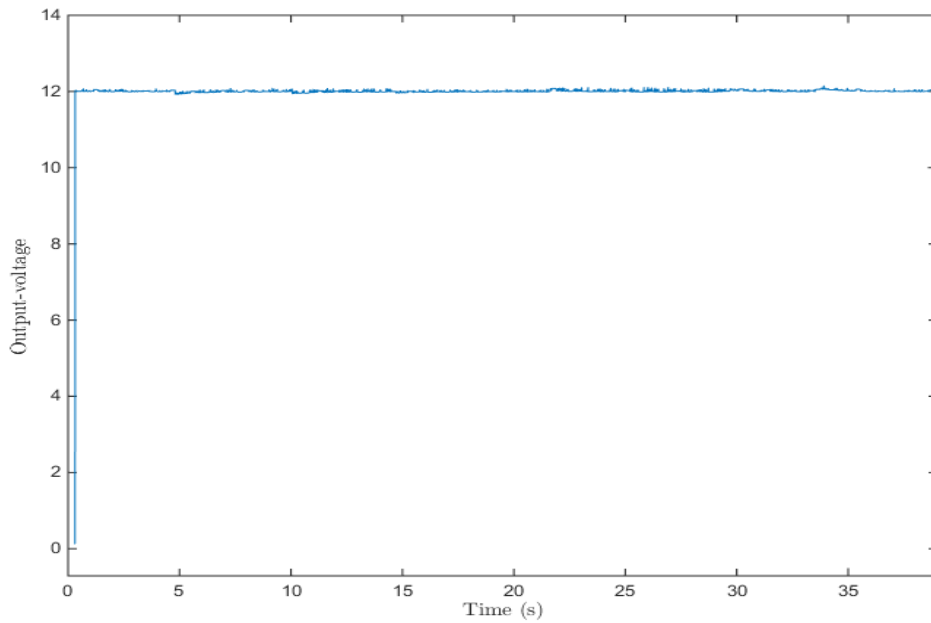


Figure III-34:Output voltage test 2

The following figure represents the duty cycle regulation:

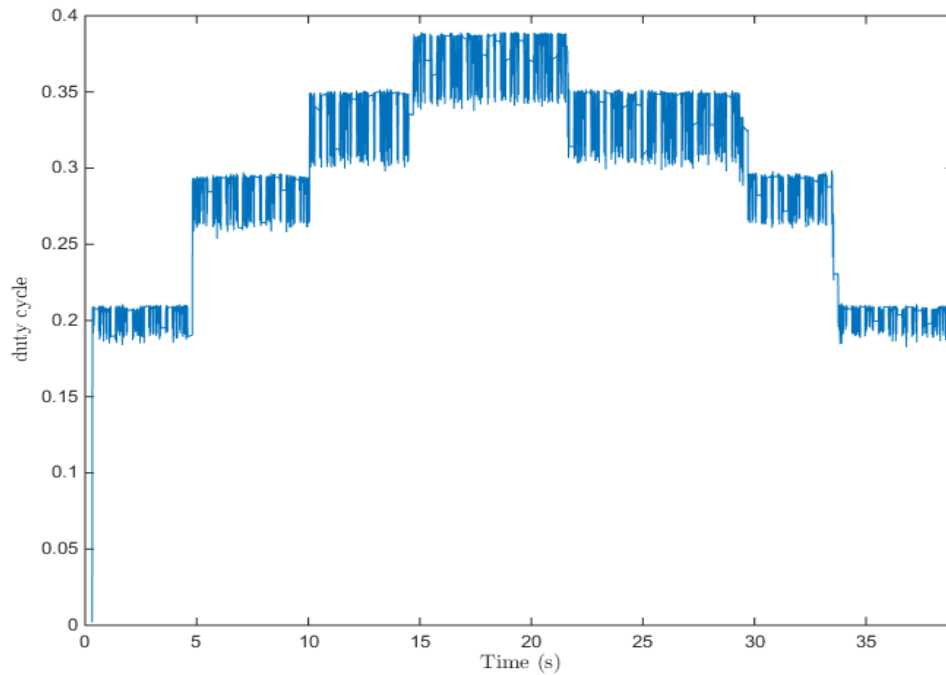


Figure III-35:Duty cycle test 2

After conducting the load variation testing, we have gained valuable insights into the robustness and adaptability of our Flyback converter design. Throughout the testing process, we intentionally adjusted the load conditions while maintaining a constant output voltage. The results reveal that our converter responded effectively to these load changes, demonstrating its ability to provide a stable output voltage even under dynamic load conditions.

We notice that the duty cycle changes by changing the load value the output is still 12V with a very small peaks the time the load is changed which means that our control is successfully working.

III.5 Conclusion

In this chapter, we embarked on a comprehensive journey through the design, simulation, realization, and control of a Flyback converter. Beginning with the design phase, we meticulously crafted a converter architecture tailored to our specific application, considering factors such as component selection, topology, and control strategy. Through detailed simulations, we scrutinized the converter's expected behavior, optimized performance, and ensured its compliance with predetermined specifications.

The transition from simulation to realization marked a critical step in our project, as we transformed theoretical designs into tangible hardware. By meticulously assembling the physical components, we were able to validate the accuracy of our simulations and gain practical insights into the converter's performance.

Furthermore, we explored the realm of control, implementing both open-loop and closed-loop configurations. This allowed us to assess the converter's response under controlled conditions, providing valuable data for system optimization and stability.

General conclusion

In conclusion, this thesis titled "Design, Implementation, and Control of Flyback Converter" has presented a comprehensive study on the Flyback converter, a widely used in power electronic devices for low-power applications. The research objectives were successfully achieved, providing valuable insights and contributions to the field of power electronics.

The thesis began by introducing the fundamentals of power supplies and highlighting the advantages of switching power supplies, with specific emphasis on the Flyback converter. The design phase involved meticulous component selection, parameter optimization, and trade-off analysis to meet the desired performance criteria, including efficiency, voltage regulation, and size constraints.

Simulation studies were conducted to validate the design and control strategies, providing a comprehensive assessment of the Flyback converter's performance. The simulation results offered valuable insights into the converter's behavior, including waveforms, efficiency estimation, and dynamic response.

The implementation phase focused on translating the designed Flyback converter into a practical realization. Considerations such as material selection, circuit layout, and thermal management were addressed to ensure reliable and efficient operation. The control system was designed and implemented using PID regulator to regulate the output voltage and maintain stability.

Through this research, a deeper understanding of the Flyback converter's operation, design principles, and control techniques has been achieved. The findings contribute of knowledge in power electronics, facilitating the development of efficient and reliable power conversion systems for low-power applications.

In conclusion, this thesis provides a significant contribution to the field by advancing the understanding of Flyback converter design, implementation, and control. The research outcomes can guide future advancements in the design of power electronic systems, enabling more efficient and sustainable energy utilization.

Perspectives

- Optimizing the Flyback converter for solar energy applications, the research contributes to sustainable energy solutions
- Explore more intricate control algorithms for the Flyback converter
- Investigate how the Flyback converter can be integrated with energy storage systems
- Examine hybrid topologies that combine the Flyback converter with other converter types

Annex

isc N-Channel MOSFET Transistor IRFP260M, IIRFP260M
• FEATURES

- Static drain-source on-resistance:
 $R_{DS(on)} \leq 40m\Omega$
- Enhancement mode:
- 100% avalanche tested
- Minimum Lot-to-Lot variations for robust device performance and reliable operation

• DESCRIPTION

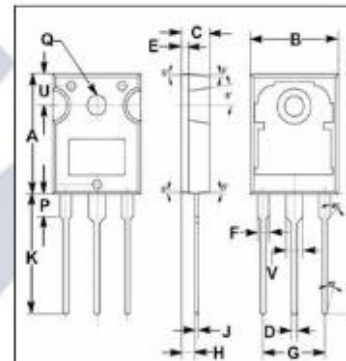
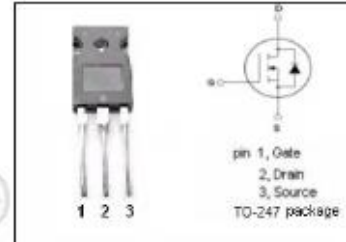
- High Speed Power Switching

• ABSOLUTE MAXIMUM RATINGS($T_a=25^\circ C$)

| SYMBOL | PARAMETER | VALUE | UNIT |
|-----------|--------------------------------------|----------|------------|
| V_{DS} | Drain-Source Voltage | 200 | V |
| V_{GS} | Gate-Source Voltage | ± 20 | V |
| I_D | Drain Current-Continuous | 50 | A |
| I_{DM} | Drain Current-Single Pulsed | 200 | A |
| P_D | Total Dissipation @ $T_c=25^\circ C$ | 300 | W |
| T_J | Max. Operating Junction Temperature | 175 | $^\circ C$ |
| T_{STG} | Storage Temperature | -55~175 | $^\circ C$ |

• THERMAL CHARACTERISTICS

| SYMBOL | PARAMETER | MAX | UNIT |
|---------------|---------------------------------------|-----|--------------|
| $R_{th(j-c)}$ | Channel-to-case thermal resistance | 0.5 | $^\circ C/W$ |
| $R_{th(j-a)}$ | Channel-to-ambient thermal resistance | 40 | $^\circ C/W$ |



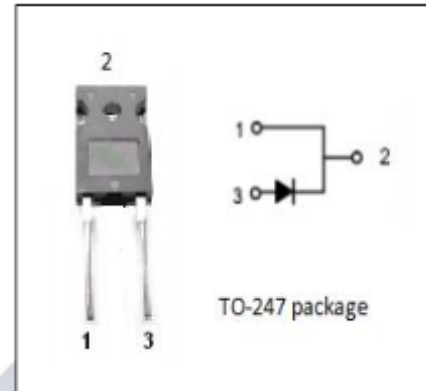
| DIM | mm | |
|-----|-------|-------|
| | MIN | MAX |
| A | 19.80 | 20.20 |
| B | 15.40 | 15.80 |
| C | 4.90 | 5.10 |
| D | 0.90 | 1.10 |
| E | 1.40 | 1.60 |
| F | 1.90 | 2.10 |
| G | 10.80 | 11.00 |
| H | 2.40 | 2.60 |
| J | 0.50 | 0.70 |
| K | 19.50 | 20.50 |
| P | 3.90 | 4.10 |
| Q | 3.30 | 3.50 |
| U | 5.20 | 5.40 |
| V | 2.90 | 3.10 |

Ultra fast Rectifier
RHRG75120
FEATURES

- With TO-247 packaging
- High performance fast recovery diode
- Low loss and soft recovery
- Low forward voltage drop
- Minimum Lot-to-Lot variations for robust device performance and reliable operation

APPLICATIONS

- Switching power supply
- Power switching circuits
- General purpose


ABSOLUTE MAXIMUM RATINGS (T_a=25 °C)

| SYMBOL | PARAMETER | VALUE | UNIT |
|--|--|-------------|------|
| V _{RRM} V _{RWM} V _R | Peak Repetitive Reverse Voltage Working Peak Reverse Voltage DC Blocking Voltage | 1200 | V |
| I _{F(AV)} | Average Rectified Forward Current @T _c =42 °C | 150 | A |
| I _{FSM} | Nonrepetitive Peak Surge Current (Surge applied at rated load conditions half-wave, single phase) | 60HZ 500 | A |
| P _D | Total Dissipation @T _c =25 °C | 190 | W |
| T _J | Junction Temperature | -85~175 | °C |
| T _{stg} | Storage Temperature Range | -85~175 | °C |

 isc website: www.iscsemi.com

1 isc & iscsemi is registered trademark

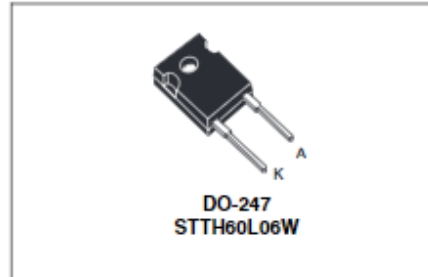


STTH60L06

TURBO 2 ULTRAFAST HIGH VOLTAGE RECTIFIER

Table 1: Main Product Characteristics

| | |
|----------------|--------|
| $I_{F(AV)}$ | 60 A |
| V_{RRM} | 600 V |
| T_J | 175°C |
| V_F (typ) | 0.95 V |
| t_{rr} (max) | 70 ns |



FEATURES AND BENEFITS

- Ultrafast switching
- Low reverse current
- Low thermal resistance
- Reduces switching & conduction losses

DESCRIPTION

The STTH60L06, which is using ST Turbo 2 600V technology, is specially suited for use in switching power supplies, and industrial applications, as rectification and discontinuous mode PFC boost diode. Thanks to its low V_F characteristics, this device exhibits high performances in free-wheeling applications.

Table 2: Order Codes

| Part Number | Marking |
|-------------|------------|
| STTH60L06W | STTH60L06W |

Table 3: Absolute Ratings (limiting values)

| Symbol | Parameter | Value | Unit |
|--------------|--|--|------|
| V_{RRM} | Repetitive peak reverse voltage | 600 | V |
| $I_{F(RMS)}$ | RMS forward current | 90 | A |
| $I_{F(AV)}$ | Average forward current | $T_c = 110^\circ\text{C} \quad \delta = 0.5$ 60 | A |
| I_{FSM} | Surge non repetitive forward current | $t_p = 10\text{ms sinusoidal}$ 400 | A |
| T_{stg} | Storage temperature range | -65 to + 175 | °C |
| T_J | Maximum operating junction temperature | 175 | °C |

Typical Power Handling Chart

| Power in Watts | | | | Pot, RS, DS | E Cores | RM, PQ, EP | UU, UI, UR | ETD, EER, EC | EFD, Planar | Toroid |
|----------------|--------|---------|---------|----------------------------|----------------------|--|----------------------|-------------------------------------|---|--|
| 20 kHz | 50 kHz | 100 kHz | 250 kHz | | | | | | | |
| 2 | 3 | 4 | 7 | 41811 RS DS PC | 41205 EE 41707 EE | 41313 EP 41812 RM 41912 RM | | | 42107 EE 41805 EE | 40907 TC 41406 TC 41303 TC 41435 TC 41304 TC 41206 TC 41506 TC 41407 TC 41405 TC 41305 TC |
| 5 | 8 | 11 | 21 | 41814 PC 42311 RS DS HS | 41808 EE | 41717 EP 42013 RM 42016 PQ 42610 PQ | | | 42019 EFD 42216 EI 42214 EI 43208 EI | 41306 TC 41607 TC 41450 TC 41410 TC 41605 TC 41610 TC 41606 TC |
| 12 | 18 | 27 | 52 | | 41810 EE 42510 EE | 42316 RM | | | | |
| 13 | 20 | 29 | 56 | 42213 PC | | 42614 PQ | | | | |
| 15 | 22 | 32 | 62 | 42318 RS DS HS | | | | | 42214 EE | |
| 18 | 28 | 40 | 78 | | | 42020 PQ | | | 42523 EFD | |
| 19 | 30 | 42 | 83 | 42616 RS DS HS | 42513 EE 42515 EI | 42120 EP 43214 PQ | 42515 UI | | 42216 EE 43618 EI 42217 EE 44008 EI | 42106 TC 41809 TC |
| 26 | 42 | 58 | 113 | | | | | | 43208 EE | 42206 TC |
| 28 | 45 | 63 | 122 | | 42520 EE | | | | 43030 EFD | |
| 30 | 49 | 67 | 131 | 42616 RS PC | | 42620 PQ | | | | 42109 TC |
| 33 | 53 | 74 | 144 | | 42515 EE | 42819 RM | | | | 42207 TC |
| 40 | 61 | 90 | 175 | | 42526 EE 43007 EE | | | | | 42506 TC |
| 42 | 70 | 94 | 183 | 43019 HS | | 42625 PQ | | | 43618 EE | |
| 48 | 75 | 108 | 210 | 42823 PC 43019 RS DS PC | 43009 EE | | 42512 UU 42515 UU | 42929 ETD | 44008 EE | 42507 TC |
| 60 | 97 | 135 | 262 | | 42530 EE 43515 EE | 43220 PQ | | 43517 EC | 43808 EI | 42212 TC |
| 70 | 110 | 157 | 306 | 43622 DS HS | | 43723 RM | 42220 UU 42530 UU | 42814 EER 42817 EER 43434 ETD | | 42508 TC 42908 TC 42712 TC |
| 105 | 160 | 235 | 460 | 43622 RS | 44011 EE 44317 EE | | | | 44308 EI 44310 EI | |
| 120 | 195 | 270 | 525 | 43622 PC | | 43230 PQ | | | 43808 EE | 43806 TC |
| 130 | 205 | 290 | 570 | | 43520 EE | 44230 RM | | 44119 EC | 43809 EE | |
| 150 | 240 | 337 | 656 | | 44016 EE 44020 EI | | | 43521 EER 43939 ETD | 44308 EE | 43113 TC 42915 TC |
| 200 | 310 | 450 | 875 | | | | | | 44310 EE | 43610 TC |

| TYPE/SIZE | ORDERING CODE | NOMINAL A ₁ (mH/1000T) | | | | | | |
|------------|------------------|-----------------------------------|-------|-------|-------|-------|-------|--------|
| | | L | R | P | F | T | J | W |
| E 9/4/2 | 0_40904EC | 280 | 493 | 540 | 650 | | 1,040 | |
| E 13/7/3 | 0_41203EC | 350 | 587 | 640 | 770 | | 1,367 | |
| E 13/7/6 | 0_41205EC | 700 | 1,467 | 1,600 | 1,950 | | 3,300 | |
| E 17/7/4 | 0_41707EC | 520 | 1,013 | 1,100 | 1,300 | | 1,900 | |
| E 19/8/5 | 0_41808EC | 550 | 1,153 | 1,253 | 1,500 | 1,500 | 2,500 | 4,293 |
| E 19/8/10 | 0_41810EC | 1,000 | 2,300 | 2,500 | 3,000 | | 5,000 | 8,600 |
| E 25/10/7 | 0_42510EC | 800 | 1,767 | 1,920 | 2,300 | | 3,700 | 7,660 |
| E 25/13/7 | 0_42513EC | 900 | 1,900 | 2,314 | 2,460 | | 4,000 | |
| E 25/16/6 | 0_42515EC | 540 | 1,153 | 1,253 | 1,500 | | 2,400 | |
| E 25/10/13 | 0_42520EC | 1,600 | 3,533 | 3,840 | 4,600 | | 7,400 | 13,813 |
| E 25/13/11 | 0_42526EC | | 2,800 | 3,512 | 4,068 | 4,068 | 5,951 | |
| E 25/16/13 | 0_42530EC | 1,070 | 2,307 | 2,507 | 3,000 | | 4,800 | 8,213 |
| E 31/15/7 | 0_43007EC | 920 | 2,060 | 2,240 | 2,700 | | 3,800 | 8,200 |
| E 31/13/9 | 0_43009EC | 1,400 | 2,893 | 3,147 | 3,780 | | 5,893 | |
| E 34/14/9 | 0_43515EC | | 2,667 | 2,907 | 3,500 | | 5,813 | 11,414 |
| E 35/21/9 | 0_43520EC | | 1,947 | 2,120 | 2,555 | | 4,240 | |

Bibliography

- [1] Cheriti Ahmed, "Électronique de puissance", note de cours, Université du Québec à Trois-Rivières, 2014.
- [2] "Complexity International, vol. 25, no. 1, 2 juin 2021.
- [3] Hong Seok Choi, "Transformer Design Considerations for Offline Flyback using Fairchild Power Switch," Fairchild Semiconductor, Document AN4140.
- [4] Miklos Csizmadia, "A Novel Feedback Linearization Control of Flyback Converter," Power Electronics and Drives, vol. 8, pp. 74-83, 2023.
- [5] Mohamed Radouane Gueffal et Abdelhak Batache, "Étude d'une alimentation à découpage type Flyback," Mémoire de master, Université de Ouargla, 2022.
- [6] "Uses, Advantages, and Working Principles of a Switching Power Supply," <https://www.monolithicpower.com/en/switching-power-supply>,
- [7]
- [8] Mojtaba Forouzesh, Yam P. Siwakoti, Saman A. Gorji, Frede Blaabjerg, and Brad Lehman, "Step Up DC-DC: A Comprehensive Review of Voltage Boosting Techniques, Topologies, and Applications," IEEE Transactions on Industrial Electronics, vol. 32, no. 12, pp. [9143-9178], décembre 2017.
- [9] Nabil Abouchabana, "Étude d'une nouvelle topologie buck-boost appliquée à un MPPT," Mémoire de magister en électronique, Alger, 2009.
- [10] Guy Seguier, Francis Labrique, Philippe Delarue, "Électronique de Puissance," Dunod, Paris, 2015.
- [11] Muhammad H. Rashid, Ph.D., "Power Electronics Handbook," Third Edition, CRC Press, Florida, USA.
- [12] Hadi Tarzamni, Ebrahim Babaei, Amirreza Zarrin Gharehkoushan, "A Full Soft Switching ZVZCS Flyback Converter Using an Active Auxiliary Cell," IEEE Transactions on Power Electronics, vol. 64, no. 2, pp. 1123-1129, 2017.
- [13] Ali Mamizadeh, Naci Genc, Mehmet Can Taneri, "Analyzing and Comparing of Variable and Constant Switching Frequency Flyback DC-DC Converter," in Proceedings of the 4th International Conference on Power Electronics and their Applications (ICPEA), 25-27 September 2019, Elazig, Turkey.
- [14] Kusumal Chalermyanont, Pairote Sangampai, Anuwat Prasertsit, Surapon Theinmontri, "High Frequency Transformer Designs for Improving Cross Regulation in Multiple-Output

- Flyback Converters" in Proceedings of the 7th International Conference on Power Electronics and Drive Systems, pp. [53-56], 2007.
- [15] Robert W. Erickson and Dragan Maksimović, "Fundamentals of Power Electronics," Third Edition, Springer, 2019.
- [16] IRES Iskender, SAEID AGHAEI Hashjin, A. Mamizadeh, "Design And Implementation Of A Six Isolated Output Flyback Converter," International Journal of Engineering, Technology, and Natural Sciences, vol. 2, pp[12-19], 2016.
- [17] "What is a Flyback Converter," Sunpower Electronics .
- [18] "Advantages and Disadvantages of Flyback Converter," RF Wireless World
- [19] "Flyback Converter," HardwareBee WikiBee,
<https://hardwarebee.com/WikiBee/flyback-converter/>
- [20] Rudy Severns, "Design of Snubbers for Power Circuits.
- [21] Fairchild Semiconductor, "Design Guidelines for RCD Snubber of Flyback Converters - Application Note AN-4147,
- [22] "UC3842/UC3843/UC3844/UC3845 SMPS Controller Datasheet," Mouser Electronics,
<https://www.mouser.com/datasheet/2/389/uc3842-uc3843-uc3844-uc3845-2294786.pdf>
- [23] Monolithic Power Systems, "How to Design a Flyback Converter in Seven Steps," Monolithic Power Systems, <https://www.monolithicpower.com/how-to-design-a-flyback-converter-in-seven-steps>
- [24] "Magnetics-2021-Ferrite-Catalog," Magnetic, Inc., www.mag-inc.com
- [25] "Switching Power Supply Design," Schmidt-Walter Schaltnetzteile, http://schmidt-walter-schaltnetzteile.de/smps_e/spw_smps_e.html
- [26] "SPICE Modeling of Magnetic Core from Datasheet," YouSpice,
<https://youspice.com/spice-modeling-of-magnetic-core-from-datasheet/>, [Accès le 17 6 2023]
- [27] Mansi Tripath "MODELLING AND ANALYSIS OF FLYBACK CONVERTER" Master of Technology In Power Systems, DELHI TECHNOLOGICAL UNIVERSITY 2022.